MERCK 默克

MILLIPLEX®

April 2021 • VOLUME 01

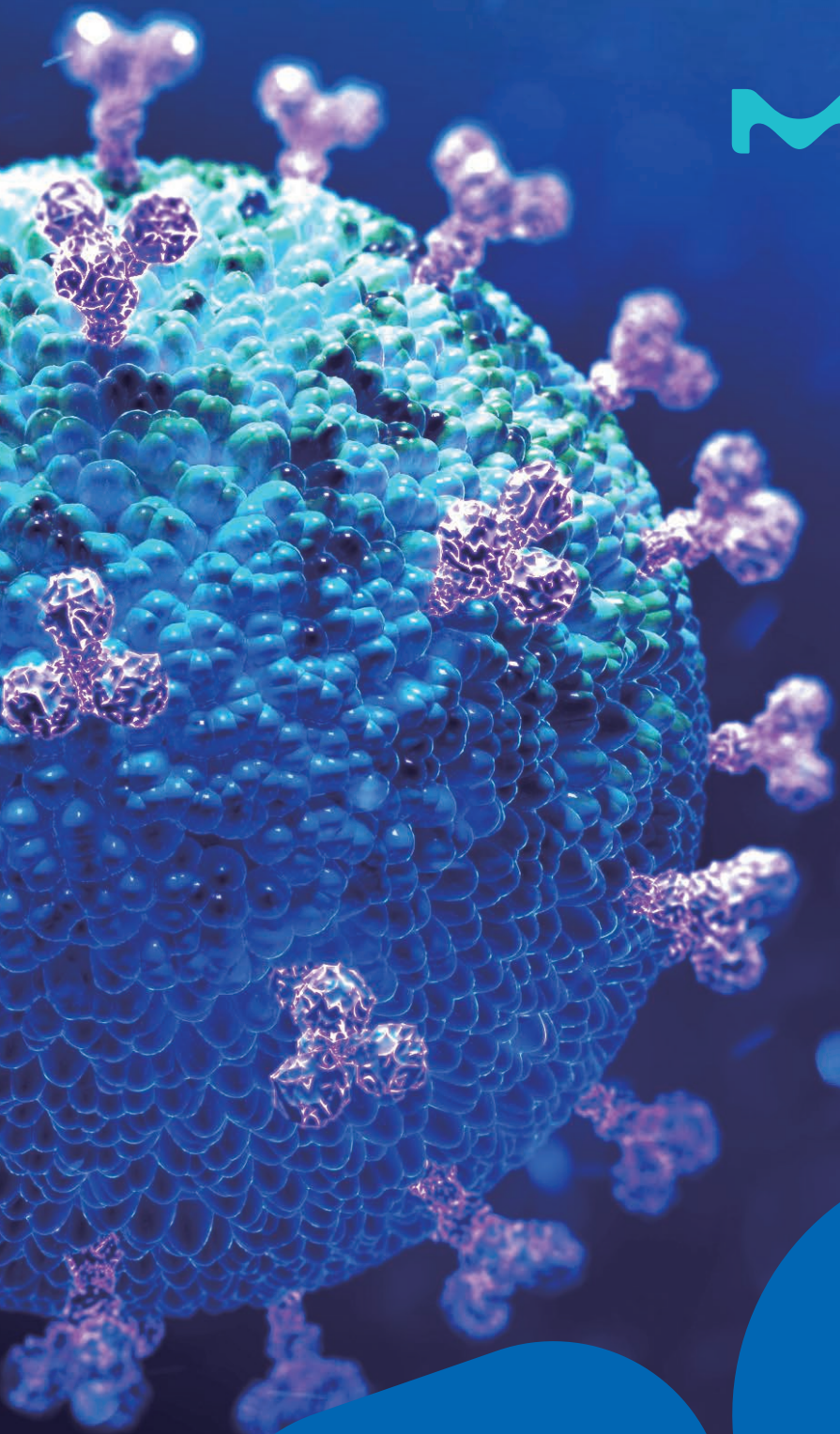

Take your RESEARCH to the NEXT LEVEL

科技改变科研生活

Millipore®

Preparation, Separation,
Filtration & Testing Products

默克生命科学业务在美国和加拿大
地区以MilliporeSigm品牌运营

contents

2021.03
VOLUME 01

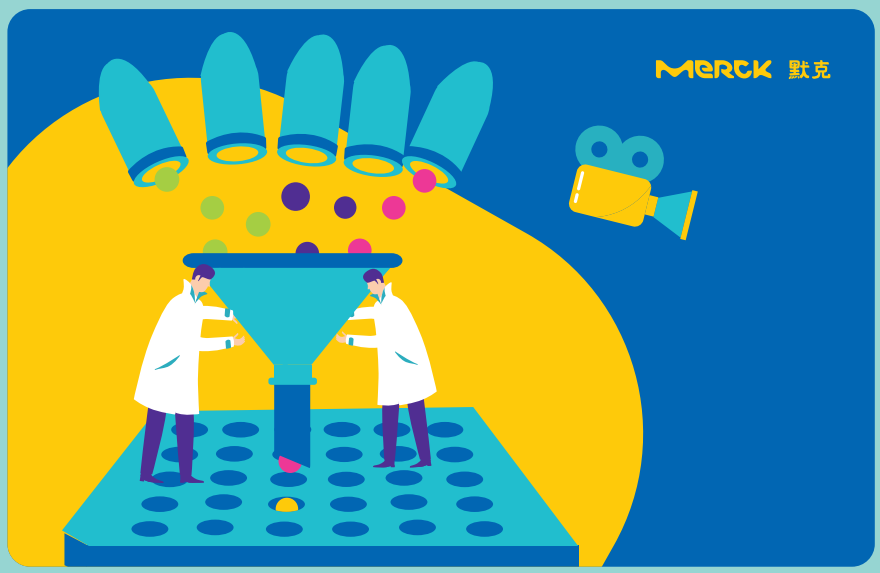

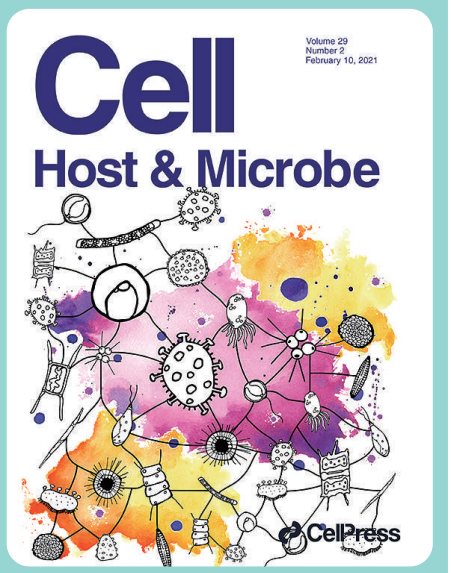

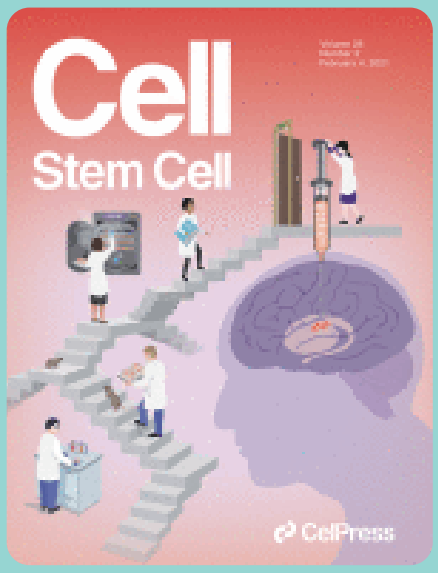

01 卷首语

默克MILLIPLEX®技术回顾

MILLIPLEX® 是基于 xMAP® 技术的液相芯片多因子检测产品，该技术采用独特的微球染色技术，通过 2-3 种荧光染料，按照不同比例对微米级的微球进行染色，可获得 1-500 种不同微球组成的液相微球悬浮芯片系统，检测时不同颜色微珠上偶联针对不同待测分析物特异性捕获抗体，通过最终荧光标记的检测抗体双抗夹心原理，使用 Luminex® 平台，轻松实现对单个样本中的多种待测分析物的精确检测。

MILLIPLEX® 做为多因子免疫检测试剂盒，可以实现百种蛋白因子的同步检测。产品设计初衷就是最大限度的为客户节约时间、节约经费、节约样本。以最快的速度、最少的时间和最低的样本需求量，发最高质量的文章。

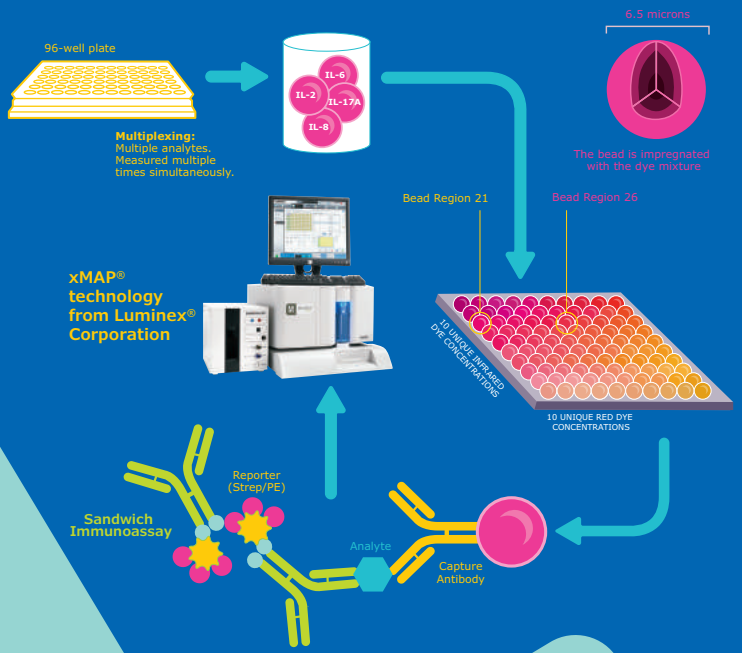

原理图示

MILLIPLEX®商品化试剂盒可以实现

< 25ul 样本

96 个样品 > 48 种因子同步检测

< 3h 实验时间

平均每板获得 > 4608 个数据

Always growing!

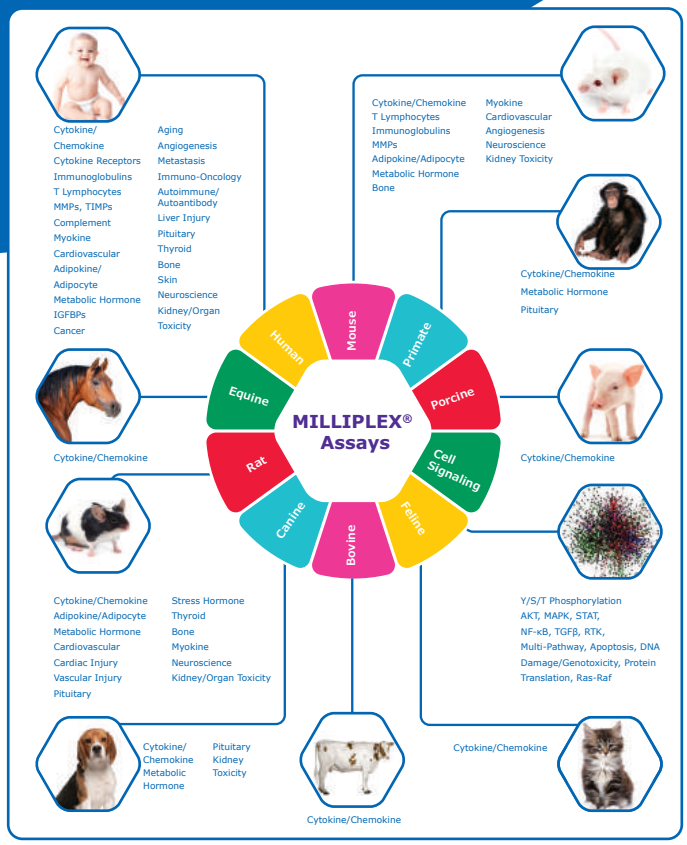

1175+

截至 2021 年 2 月，默克 MILLIPLEX® 试剂盒已有千种因子可选

10

覆盖十种属，分别是Human, Mouse, Rat, Bovine, Canine, Equine, Feline, Non-Human Primate, Ovine, Porcine

定制服务

除此之外，默克也提供灵活的试剂盒定制服务，满足更多的因子组合需求

14250+

截至 2021 年 2 月，
使用默克 MILLIPLEX® 试剂盒的用户，
已发表上万篇文献

02 新品速递

MILLIPLEX® SARS-CoV-2 antigens detection assay

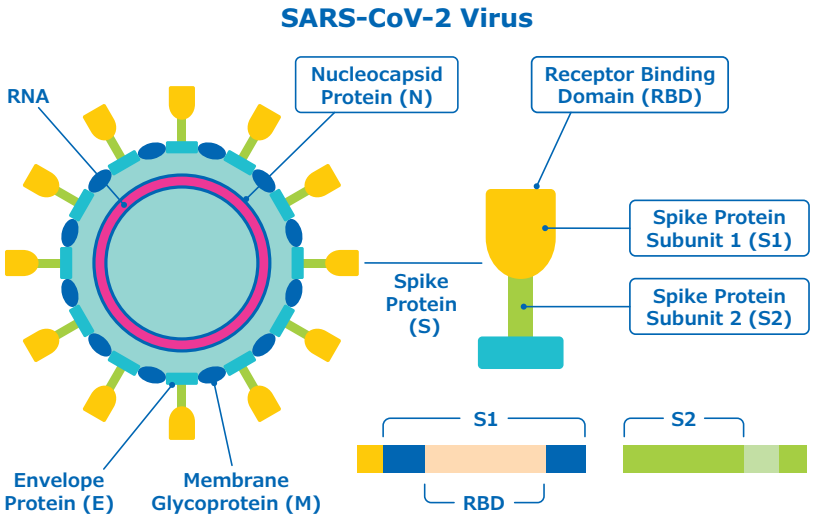

应对新冠来袭，默克 MILLIPLE® 及时上新 SARS-CoV-2 检测试剂盒，助力新冠检测与疫苗开发。

SARS-CoV-2 试剂盒可以检测 IgA、IgM 或 IgG 抗体，每个试剂盒都实现抗原 S1、S2、RBD 和 N 蛋白同步检测。用户可以需要选择全部或一部分分析物。每个试剂盒包含所有试剂和 96 孔板进行检测所需。

每个试剂盒都包含一组阳性质控和一个阴性质控品，用于试剂盒性能检测。板内 CV 控制在 15% (8 reportable results)，板间 CV 在 20% 以内(across 4 different assays)。

这些 MILLIPLEX® 试剂盒在符合 ISO 9001:2015 生产标准，仅用于研究，不用于诊断程序。

MILLIPLEX® Assay Kits 96-well Plate Format	Cat. No.
SARS-CoV-2 Antigen Panel 1 IgM	**HC19SERM1-85K**
SARS-CoV-2 Antigen Panel 1 IgG	**HC19SERG1-85K**
SARS-CoV-2 Antigen Panel 1 IgA	**HC19SERA1-85K**
Available Analytes for Each Panel	
SARS-CoV-2 Spike Subunit 1 (S1)	
SARS-CoV-2 Spike Subunit 2 (S2)	
SARS-CoV-2 Receptor Binding Domain (RBD)	
SARS-CoV-2 Nucleocapsid Protein (N)	

For Research Use Only. Not For Use In Diagnostic Procedures.

Table 1. MILLIPLEX® Assay Kits for COVID-19 Research.

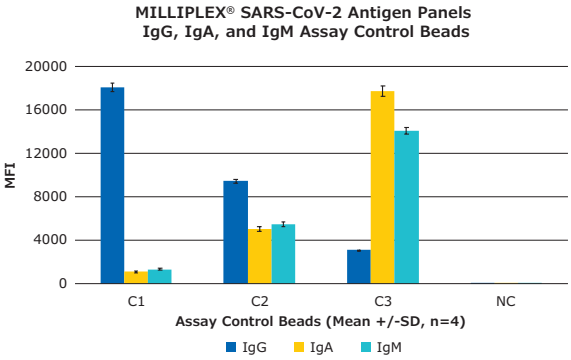

48 to 1, larger & customizable

MILLIPLEX® Human Panel A - 48 plex

默克生命科学全新推出 MILLIPLEX® Human Cytokine/Chemokine/Growth Factor Panel A，为您带来全新 48 个免疫细胞因子组合的检测试剂盒，您可以在 1-48 个因子之间任意组合，同时也可以选择 48 因子及 38 因子预混包装试剂盒。默克免疫检测解决方案，只为满足您多样的免疫检测需求。

MILLIPLEX® Human Cytokine/Chemokine/ Growth Factor Panel A

(Cat. Nos. HCYTA-60K*;
38因子预混包装: HCYTA-60K-PX38;
48因子预混包装: HCYTA-60K-PX48)
*提供1-48因子任意组合因子定制预混。

可检测因子：见下方表格
可检测样本类型：血清，血浆，组织 / 细胞裂解液，细胞培养上清
标准曲线：为每个因子都进行特定优化，可以得到更可靠的检测结果，还有批次间一致性检测，是 MILLIPLEX® 检测数据一贯的稳定的保证。

48个因子的标准曲线示例：

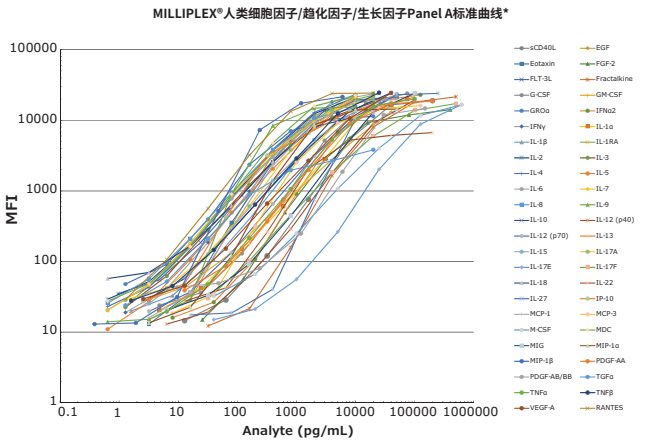

*HCYTA-60K标准曲线检测示例数据采用4°C，16-18小时过夜孵育检测方案

使用值得您信赖的MILLIPLEX®构建数据分析规范，确保随着时间的推移，检测性能保持一致不变。

Analyte	Standard Curve Range (pg/mL)	Sensitivity: minDC (pg/mL)*
sCD40L	13 – 200,000	5.65
EGF°	3 – 50,000	3.20
Eotaxin°	3 – 50,000	3.08
FGF-2	26 – 400,000	22.30
FLT-3L	0.96 – 15,000	0.84
Fractalkine	32 – 500,000	29.75
G-CSF°	4.8 – 75,000	3.76
GM-CSF°	2.6 – 40,000	1.55
GROα	1.3 – 20,000	1.05
IFNα2°	8 – 125,000	6.56
IFNγ°	1.3 – 20,000	0.86
IL-1α°	4.8 – 75,000	2.27
IL-1β°	1.6 – 25,000	0.52
IL-1RA°	1.6 – 25,000	1.29
IL-2°	0.64 – 10,000	0.28
IL-3°	1.3 – 20,000	0.28
IL-4°	0.64 – 10,000	0.20
IL-5°	0.64 – 10,000	0.17
IL-6°	0.64 – 10,000	0.14
IL-7°	0.64 – 10,000	0.14
IL-8°	0.64 – 10,000	0.52
IL-9	0.64 – 10,000	3.05
IL-10°	2.6 – 40,000	0.91
IL-12 (p40)°	6.4 – 100,000	3.24

Analyte	Standard Curve Range (pg/mL)	Sensitivity: minDC (pg/mL)*
IL-12 (p70)°	3 – 50,000	0.88
IL-13°	6.4 – 100,000	2.58
IL-15°	3 – 50,000	0.74
IL-17A°	1.3 – 20,000	0.71
IL-17E/IL-25°	40 – 625,000	19.77
IL-17F°	32 – 500,000	28.63
IL-18°	0.64 – 10,000	0.53
IL-22°	13 – 200,000	12.68
IL-27	16 – 250,000	50.78
IP-10/CXCL10°	2.6 – 40,000	2.13
MCP-1°	3 – 50,000	3.05
MCP-3	8 – 125,000	8.61
M-CSF°	40 – 625,000	31.95
MDC	0.64 – 10,000	0.42
MIG°	6.4 – 100,000	3.98
MIP-1α°	3 – 50,000	3.82
MIP-1β°	0.38 – 6,000	0.37
PDGF-AA°	13 – 200,000	10.33
PDGF-AB/BB°	9.6 – 150,000	16.39
RANTES°	1.3 – 20,000	1.58
TGFα	1.3 – 20,000	0.97
TNFα°	6.4 – 100,000	5.39
TNFβ°	1.6 – 25,000	0.80
VEGF-A°	2.6 – 40,000	0.98

*检测灵敏度(minDC，或最小可检出浓度)计算使用过夜检测实验方案n=8，数据使用MILLIPLEX®Analyst 5.1软件分析，查看我们的试剂盒操作手册获取更多信息。
°38因子预混试剂盒检测数据包含在其中

03 文献导览

严重急性呼吸综合征冠状病毒 2 型(SARS-CoV-2)的出现导致了 COVID-19 的大流行，抗体测试对于确定接触病毒的人和预测疾病免疫性是必不可少的。文章对 183 名 COVID-19 患者（其中 68 名患者使用呼吸机）和 41 名对照者血浆进行检测；使用 MILLIPLEX® SARS-CoV-2 检测试剂盒检测血浆中争对 SARS-CoV-2 S1、S2、RBD 和 N 蛋白的 IgG、IgA 和 IgM 抗体水平，使用 MILLIPLEX® Panel A 48 因子检测试剂盒检测血浆中细胞因子水平。研究发现，抗 SARS-CoV-2 抗体水平在症状出现后几天内升高，一周内达到 90% 以上的敏感性和特异性，在需要机械通气的患者中最高。抗体水平与病毒载量呈负相关，抗 SARS-CoV-2 抗体水平最高的患者鼻咽的病毒载量最低。高血浆 IL-10 与低抗 SARS-CoV-2 抗体存在相关性，这种细胞因子在 COVID-19 的体液免疫应答中具有潜在的抑制作用。

IgG Antibodies against SARS-CoV-2 Correlate with Days from Symptom Onset, Viral Load and 1 IL-10

COVID-19 研究

Department of Medicine, University of Virginia Health System, Charlottesville, VA, USA
Posted December 7, 2020
https://doi.org/10.1101/2020.12.05.20244541

Abstract

The emergence of severe acute respiratory syndrome coronavirus 2 (SARS-CoV-2) has resulted in a pandemic of the respiratory disease coronavirus disease 2019 (COVID-19). Antibody testing is essential to identify persons exposed to the virus and potentially in predicting disease immunity. 183 COVID-19 patients (68 of whom required mechanical ventilation) and 41 controls were tested for plasma IgG, IgA and IgM against the SARS-CoV-2 S1, S2, receptor binding domain (RBD) and N proteins using the MILLIPLEX® SARS-CoV-2 Antigen Panel. Plasma cytokines were concurrently measured using the MILLIPLEX® MAP Human Cytokine/ Chemokine/Growth Factor Panel A. As expected, the 183 COVID-19 positive patients had high levels of IgG, IgA and IgM anti-SARS-CoV-2 antibodies against each of the viral proteins. Sensitivity of anti-S1 IgG increased from 60% to 93% one week after symptom onset. S1-IgG and S1-IgA had specificities of 98% compared to the 41 COVID-19 negative patients. The 68 ventilated COVID-19 positive patients had higher antibody levels than the 115 COVID-19 positive patients who were not ventilated. IgG antibody levels against S1 protein had the strongest positive correlation to days from symptom onset. There were no statistically significant differences in IgG, IgA and IgM antibodies against S1 based on age. We found that patients with the highest levels of anti-SARS-CoV-2 antibodies had the lowest viral load in the nasopharynx. Finally, there was a correlation of high plasma IL-10 with low anti-SARS-CoV-2 antibodies. Anti-SARS-CoV-2 antibody levels, as measured by a novel antigen panel, increased within days after symptom onset, achieving > 90% sensitivity and specificity within one week, and were highest in patients who required mechanical ventilation. Antibody levels were inversely associated with viral load but did not differ as a function of age. The correlation of high IL-10 with low antibody response suggests a potentially suppressive role of this cytokine in the humoral immune response in COVID-19.

Figure 1

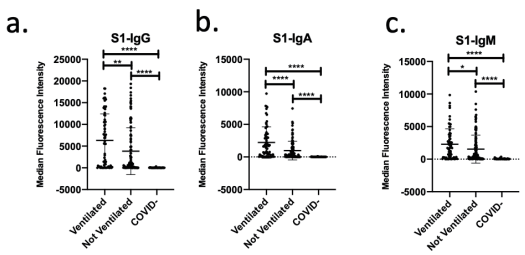

抗S1的IgG、IgA和IgM抗体在不同年龄组中浓度，没有显著统计学差异。

Figure 1: IgG, IgA and IgM antibody response to SARS-CoV-2 S1 increased in ventilated patients. (a-c) IgG, IgA and IgM antibody responses to SARS-CoV-2 S1 in ventilated COVID-19 positive patients (n=68), not ventilated COVID-19 positive patients (n=115), and COVID-19 negative patients (n=41). ****p<0.0001, ***p<0.001, **p<0.01, *p<0.05

Figure 2

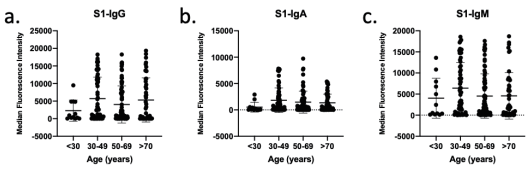

Figure 2: IgG, IgA and IgM antibody response to SARS-CoV-2 S1 and age.
(a-c) IgG, IgA and IgM antibody responses to SARS-CoV-2 S1 in patients less than 30 years old (n=12), 30-49 years old (n=53), 50-69 years old (n=70) and greater than 70 years old (n=47).

Figure 3

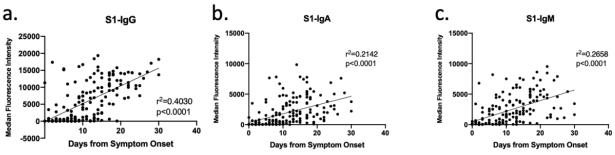

Figure 4

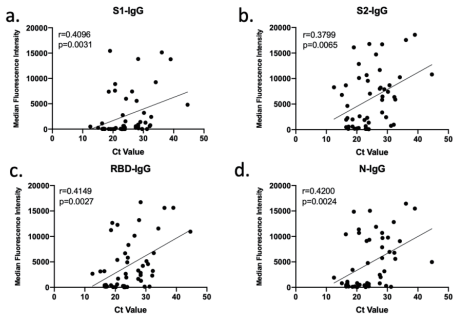

抗S1蛋白IgG抗体水平与发病天数呈正相关，抗S1-IgG的检出水平在症状出现一周后由60%提高到93%。

Figure 3: Correlation of IgG, IgA and IgM antibodies against SARS-CoV-2 S1 and days from symptom onset.
(a-c) Correlation of IgG, IgA and IgM antibodies against SARS-CoV-2 S1 and days from symptom onset (168 samples from 123 patients).

Figure 4: Correlation of IgG Antibodies and SARS-CoV-2 Ct Value.
(a-d) Correlation of IgG antibodies against SARS-CoV-2 S1, S2, RBD and N and SARS-CoV-2 Ct Value (n=50).

Figure 5

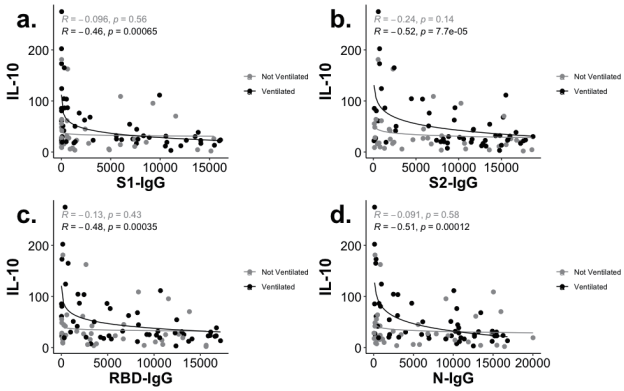

高血浆IL-10与低抗SARS-CoV-2抗体存在相关性。

Figure 5: Correlation of IgG Antibodies and Il-10.
(a-d) Correlation of anti-S1, S2, RBD and N IgG antibodies and Il-10 in ventilated (black, n=51) and not ventilated (grey, n=40) COVID-19 positive patients.

MILLIPLEX ®多因子试剂盒信息：

SARS-CoV-2 Antigen Panel 1 IgA NEW **

(Cat. No. HC19SERA1-85K)

SARS-CoV-2 N	SARS-CoV-2 Spike S1
SARS-CoV-2 RBD	SARS-CoV-2 Spike S2

SARS-CoV-2 Antigen Panel 1 IgG NEW **

(Cat. No. HC19SERG1-85K)

SARS-CoV-2 N	SARS-CoV-2 Spike S1
SARS-CoV-2 RBD	SARS-CoV-2 Spike S2

SARS-CoV-2 Antigen Panel 1 IgM NEW **

(Cat. No. HC19SERM1-85K)

SARS-CoV-2 N	SARS-CoV-2 Spike S1
SARS-CoV-2 RBD	SARS-CoV-2 Spike S2

Human Cytokine/Chemokine/ Growth Factor Panel A

48 (Cat. No. HCYTA-60K-PX48)

sCD40L	IL-13♦
EGF♦	IL-15♦
Eotaxin/CCL11♦	IL-17A/CTLA8♦
FGF-2/FGF-basic	IL-17E/IL-25♦
Flt3 Ligand	IL-17F♦
Fractalkine/CX3CL1	IL-18♦
G-CSF♦	IL-22♦
GM-CSF♦	IL-27
GROα	IP-10/CXCL10♦
IFNα2♦	MCP-1/CCL2♦
IFNγ♦	MCP-3/CCL7
IL-1α♦	M-CSF♦
IL-1β♦	MDC/CCL22
IL-1RA♦	MIG/CXCL9♦
IL-2♦	MIP-1α/CCL3♦
IL-3♦	MIP-1β/CCL4♦
IL-4♦	PDGF-AA♦
IL-5♦	PDGF-AB/BB♦
IL-6♦	RANTES/CCL5♦▲
IL-7♦	TGFα
IL-8/CXCL8♦	TNFα♦
IL-9	TNFβ/Lymphotoxin-α (LTA)♦
IL-10♦	VEGF-A♦
IL-12 (p40)♦	
IL-12 (p70)♦	

扫我试用

疾病机理的研究常常需要在动物模型上进行，进而推进医学对策的开发和试验。本文研究人员将恒河猴作为模式动物建立新型冠状病毒病模型，对发病机制进行研究。研究发现，在 SARS-CoV-2 感染引起的呼吸系统疾病可以持续 8-16 天，同时肺部 X 光成像观察到恒河猴出现了肺浸润，在所有动物的鼻咽拭子和支气管肺泡灌洗液中均检测到高病毒载量。

Respiratory disease in rhesus macaques inoculated with SARS-CoV-2

COVID-19 研究

Laboratory of Virology, National Institute of Allergy and Infectious Diseases, National Institutes of Health, Hamilton, MT, USA.

Published: 12 May 2020
https://doi.org/10.1038/s41586-020-2324-7

Abstract

An outbreak of coronavirus disease 2019 (COVID-19), which is caused by a novel coronavirus (named SARS-CoV-2) and has a case fatality rate of approximately 2%, started in Wuhan (China) in December 2019. Following an unprecedented global spread3, the World Health Organization declared COVID-19 a pandemic on 11 March 2020. Although data on COVID-19 in humans are emerging at a steady pace, some aspects of the pathogenesis of SARS-CoV-2 can be studied in detail only in animal models, in which repeated sampling and tissue collection is possible. Here we show that SARS-CoV-2 causes a respiratory disease in rhesus macaques that lasts between 8 and 16 days. Pulmonary infiltrates, which are a hallmark of COVID-19 in humans, were visible in lung radiographs. We detected high viral loads in swabs from the nose and throat of all of the macaques, as well as in bronchoalveolar lavages; in one macaque, we observed prolonged rectal shedding. Together, the rhesus macaque recapitulates the moderate disease that has been observed in the majority of human cases of COVID-19. The establishment of the rhesus macaque as a model of COVID-19 will increase our understanding of the pathogenesis of this disease, and aid in the development and testing of medical countermeasures.

IF: 40.137

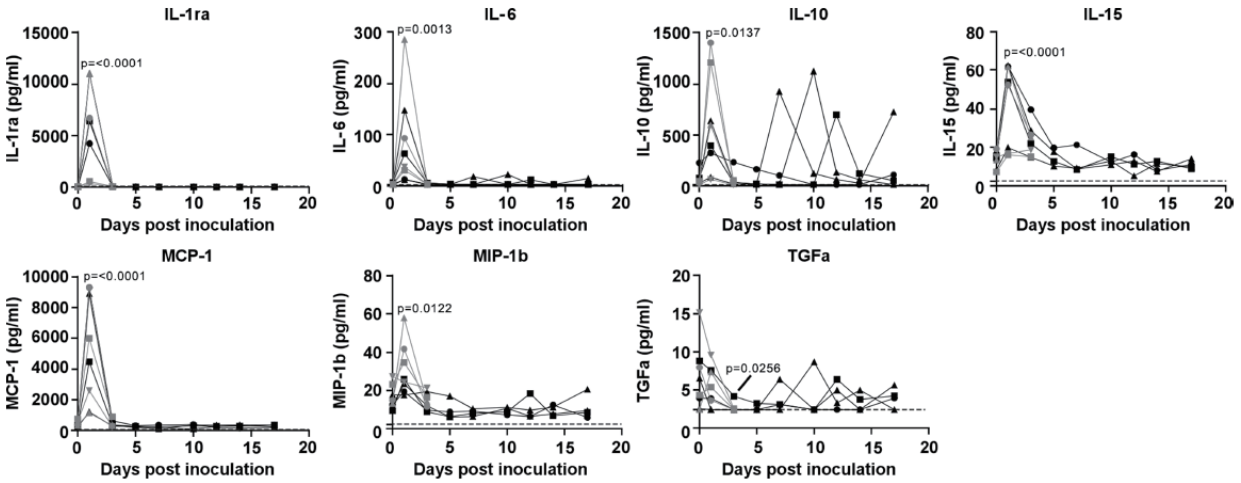

测定 SARS-CoV-2 感染后，不同时间点恒河猴血清中 23 种细胞因子和趋化因子的水平。其中 IL-1ra，IL-6, IL-10, IL-15, MCP-1, MIP-1b，TNFa 与感染前相比，有统计学显著性差异 (单向方差分析)。

Fig. 3 | Cytokine and chemokine levels in the serum of rhesus macaques infected with SARS-CoV-2. The levels of 23 cytokines and chemokines were determined in serum at different time points after inoculation. Levels are displayed only for those cytokines and chemokines for which statistically significant (one-way analysis of variance) differences were observed compared to levels on the day of inoculation. The lower limit of detection is indicated with a dotted line. Serum samples were analysed in duplicate from each macaque for each time point; n = 8 macaques at 0, 1, and 3 dpi and n = 4 macaques thereafter.

MILLIPLEX ®多因子试剂盒信息：

Non-Human Primate Cytokine/Chemokine Panel (Cat. No. PCYTMG-40K-PX23)

Non-Human Primate Cytokine/Chemokine Panel 1

(Cat. No. PRCYTOMAG-40K)
23 (Cat. No. PCYTMG-40K-PX23)
23 (Bulk Cat. No. PRCYMAG40PMX23BK)

sCD40L	IL-12/23 (p40)
G-CSF	IL-13
GM-CSF	IL-15
IFNγ	IL-17A/CTLA8
IL-1β	IL-18
IL-1Ra	MCP-1/CCL2
IL-2	MIP-1α/CCL3
IL-4	MIP-1β/CCL4
IL-5	TGFα
IL-6	TNFα
IL-8/CXCL8	VEGF-A
IL-10	

扫我咨询

2020 年初爆发的新冠疫情给全球带来了巨大冲击，随着疫情的蔓延，新冠病毒的基因组正在不断发生突变。文章选取来自于四川与武汉的临床样本，通过对分离的 SARS-CoV-2 测序与生信分析在众多突变中筛选出 35 个复发性的基因突变，再结合临床表型最终确证这些突变中 Nsp1 编码区 500-532 位的缺失更高频的发生在临床症状不严重的病人当中；文章使用 Milliplex 对病人血浆中多种细胞因子进行含量检测，发现 Nsp1 编码区的缺失最终导致血浆中干扰素 -β (IFN-β) 的含量降低，I 型干扰素信号通路抑制，病人临床症状较为轻微，为针对 SARS-CoV-2 的药物研发提供了依据。

Genomic monitoring of SARS-CoV-2 uncovers an Nsp1 deletion variant that modulates type I interferon response

COVID-19 研究

Department of Laboratory Medicine, State Key Laboratory of Biotherapy, West China Hospital, Sichuan University and Collaborative Innovation Center for Biotherapy, Chengdu, China
Department of Laboratory Medicine and Department of Pediatric Infectious Diseases, Key Laboratory of Birth Defects and Related Diseases of Women and Children of MOE, West China Second University Hospital, Sichuan University, Chengdu, China
Department of Respiratory and Critical Care Medicine, Frontier Science Center of Disease Molecular Network, West China Hospital, Sichuan University, Chengdu, China
Department of Clinical Laboratory, Zhongnan Hospital of Wuhan University, Wuhan, Hubei, China

Available online 29 January 2021
https://doi.org/10.1016/j.chom.2021.01.015

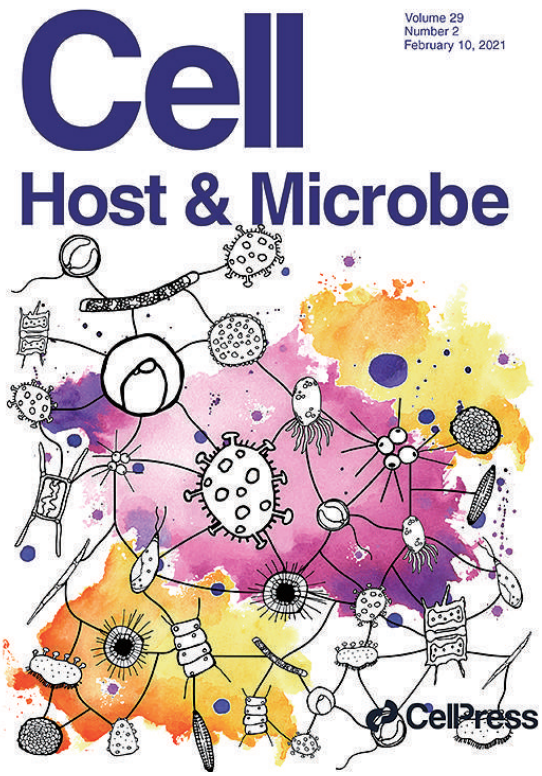

Abstract

The SARS-CoV-2 virus, the causative agent of COVID-19, is undergoing constant mutation. Here, we utilized an integrative approach combining epidemiology, virus genome sequencing, clinical phenotyping, and experimental validation to locate mutations of clinical importance. We identified 35 recurrent variants, some of which are associated with clinical phenotypes related to severity. One variant, containing a deletion in the Nsp1-coding region (Δ500-532), was found in more than 20% of our sequenced samples and associates with higher RT-PCR cycle thresholds and lower serum IFN-β levels of infected patients. Deletion variants in this locus were found in 37 countries worldwide, and viruses isolated from clinical samples or engineered by reverse genetics with related deletions in Nsp1 also induce lower IFN-β responses in infected Calu-3 cells. Taken together, our virologic surveillance characterizes recurrent genetic diversity and identified mutations in Nsp1 of biological and clinical importance, which collectively may aid molecular diagnostics and drug design.

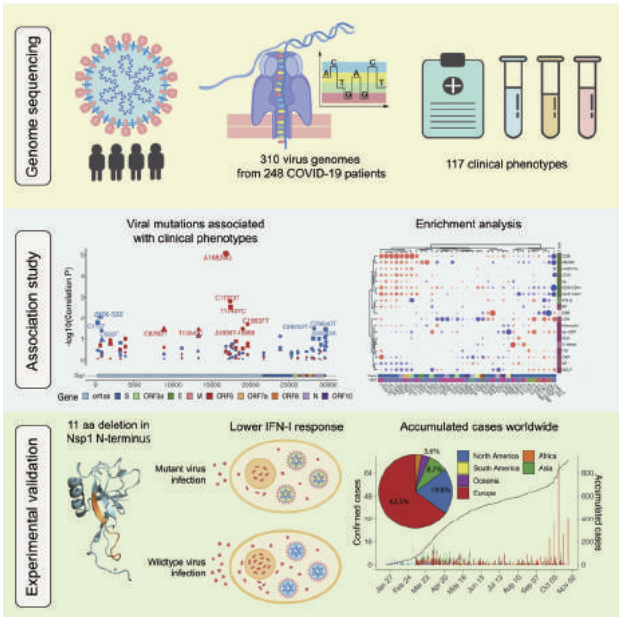

IF: 15.75

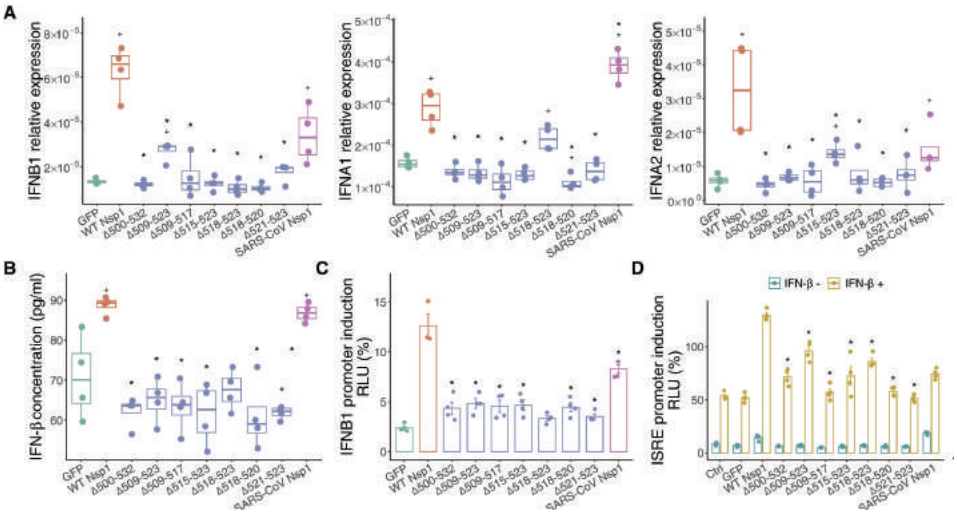

在转染的HEK293T和A549（人肺细胞系）细胞中，所有缺失变体在转录和蛋白质水平上均显示IFN-I应答降低。

Fig 6. Nsp1 mutants downregulate IFN-1 response
(B) Concentration of IFN-β in the supernatant of Nsp1-expressing A549 cells. GFP and SARS-CoV Nsp1 were used as negative and positive controls. Each dot represents a single biological replicate. Median and range of 75th percentile are also shown in the boxplots. *indicates statistical significance between mutant and WT Nsp1, and +indicates significance between GFP controls. Mann-Whitney U test was performed.

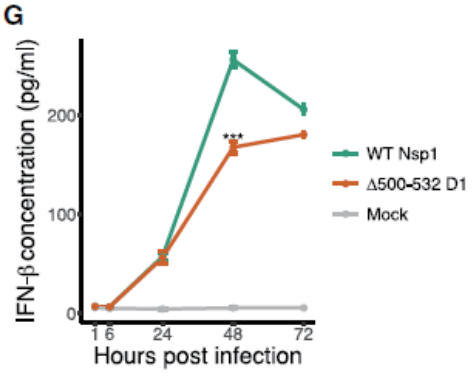

感染突变体rSARS-CoV-2的Calu-3细胞上清中IFN-b的浓度也降低

Figure 7. Growth kinetics and regulation of IFN-I response in wild-type and Nsp1 deletion virion
(G) Concentration of IFN-b in the supernatant of infected Calu-3 cells. Mean and SEM are shown. Significance betweenWT and mutant viruses was indicated; *p <0.05, **p < 0.01, and ***p < 0.001. Multiple t tests were performed.

MILLIPLEX ®多因子试剂盒信息：

Human Cytokine/Chemokine/ Growth Factor Panel A

扫我试用

(Cat. No. HCYTA-60K)
38 (Cat. No. HCYTA-60K-PX38)♦
48 (Cat. No. HCYTA-60K-PX48)

sCD40L	IL-13♦
EGF♦	IL-15♦
Eotaxin/CCL11♦	IL-17A/CTLA8♦
FGF-2/FGF-basic	IL-17E/IL-25♦
Flt3 Ligand	IL-17F♦
Fractalkine/CX3CL1	IL-18♦
G-CSF♦	IL-22♦
GM-CSF♦	IL-27
GROα	IP-10/CXCL10♦
IFNα2♦	MCP-1/CCL2♦
IFNγ♦	MCP-3/CCL7
IL-1α♦	M-CSF♦
IL-1β♦	MDC/CCL22
IL-1RA♦	MIG/CXCL9♦
IL-2♦	MIP-1α/CCL3♦
IL-3♦	MIP-1β/CCL4♦
IL-4♦	PDGF-AA♦
IL-5♦	PDGF-AB/BB♦
IL-6♦	RANTES/CCL5♦▲
IL-7♦	TGFα
IL-8/CXCL8♦	TNFα♦
IL-9	TNFβ/Lymphotoxin-α (LTA)♦
IL-10♦	VEGF-A♦
IL-12 (p40)♦	
IL-12 (p70)♦	

Human Th17

(Cat. No. HTH17MAG-14K)
25 (Cat. No. HT17MG-14K-PX25)

GM-CSF	IL-17E/IL-25
IFNγ	IL-17F
IL-1β	IL-21
IL-2	IL-22
IL-4	IL-23
IL-5	IL-27
IL-6	IL-28A/IFNλ2
IL-9	IL-31
IL-10	IL-33/NF-HEV (mature)
IL-12 (p70)	MIP-3α/CCL20
IL-13	TNFα
IL-15	TNFβ/Lymphotoxin-α (LTA)
IL-17A/CTLA8	

文章使用 MILLIPLEX 技术检测了恒河猴被新冠病毒感染后，肺组织或肠道组织中 23 个炎性细胞因子的表达情况，揭示了肠道也是新冠病毒感染的可能途径之一，对于肠道系统在新冠发病和传播过程中起到的作用,需要在新冠的预防和治疗过程中给予关注。

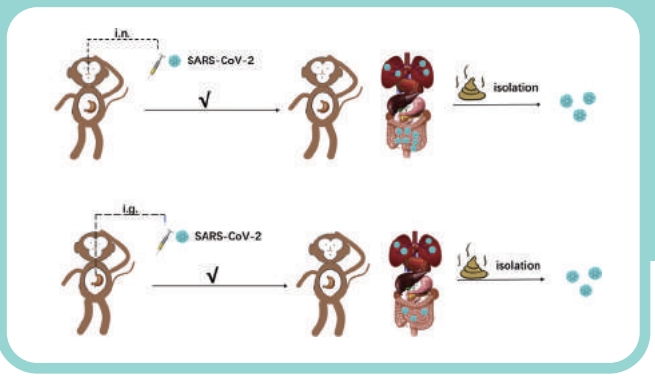

The Gastrointestinal Tract Is an Alternative Route for SARS-CoV-2 Infection in a Nonhuman Primate Model

COVID-19 研究

National Kunming High-Level Biosafety Primate Research Center, Institute of Medical Biology, Chinese Academy of Medical Sciences and Peking Union Medical College, Yunnan, China

Available online 9 December 2020
https://doi.org/10.1053/j.gastro.2020.12.001

Abstract

BACKGROUND & AIMS: Gastrointestinal (GI) manifestations have been increasingly reported in patients with coronavirus disease 2019 (COVID-19). However, the roles of the GI tract in severe acute respiratory syndrome coronavirus 2 (SARS-CoV-2) infection are not fully understood. We investigated how the GI tract is involved in SARS-CoV-2 infection to elucidate the pathogenesis of COVID-19. METHODS: Our previously established nonhuman primate (NHP) model of COVID-19 was modified in this study to test our hypothesis. Rhesus monkeys were infected with an intragastric or intranasal challenge with SARS-CoV-2. Clinical signs were recorded after infection. Viral genomic RNA was quantified by quantitative reverse transcription polymerase chain reaction. Host responses to SARS-CoV-2 infection were evaluated by examining inflammatory cytokines, macrophages, histopathology, and mucin barrier integrity. RESULTS: Intranasal inoculation with SARS-CoV-2 led to infections and pathologic changes not only in respiratory tissues but also in digestive tissues. Expectedly, intragastric inoculation with SARS-CoV-2 resulted in the productive infection of digestive tissues and inflammation in both the lung and digestive tissues. Inflammatory cytokines were induced by both types of inoculation with SARS-CoV-2, consistent with the increased expression of CD68. Immunohistochemistry and Alcian blue/periodic acid–Schiff staining showed decreased Ki67, increased cleaved caspase 3, and decreased numbers of mucin-containing goblet cells, suggesting that the inflammation induced by these 2 types of inoculation with SARS-CoV-2 impaired the GI barrier and caused severe infections. CONCLUSIONS: Both intranasal and intragastric inoculation with SARS-CoV-2 caused pneumonia and GI dysfunction in our rhesus monkey model. Inflammatory cytokines are possible connections for the pathogenesis of SARS-CoV-2 between the respiratory and digestive systems.

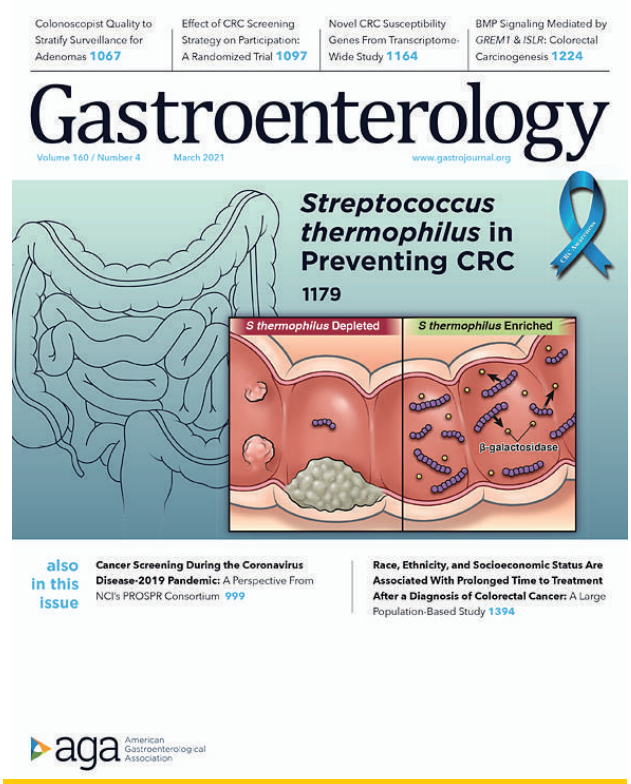

IF: 14.88

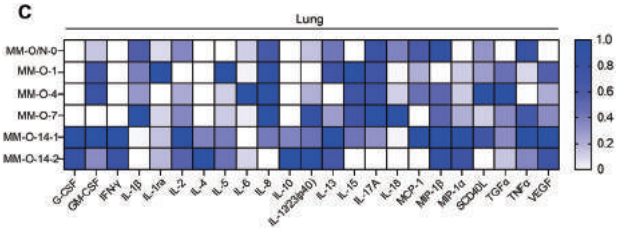

抗S1蛋白IgG抗体水平与发病天数呈正相关，抗S1-IgG的检出水平在症状出现一周后由60%提高到93%。

Figure 3: Correlation of IgG, IgA and IgM antibodies against SARS-CoV-2 S1 and days from symptom onset.
(a-c) Correlation of IgG, IgA and IgM antibodies against SARS-CoV-2 S1 and days from symptom onset (168 samples from 123 patients).

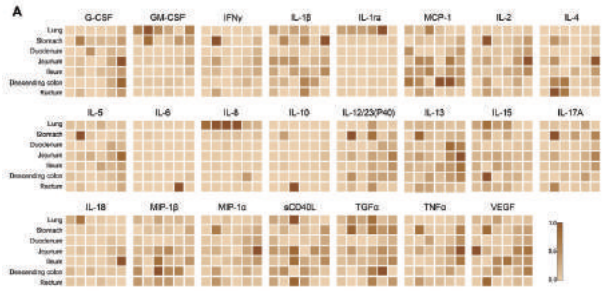

SARS-CoV-2感染可引起消化系统炎症反应。

Figure 3. Inflammatory responses in the digestive system and virus shedding in rhesus monkeys intranasally challenged with SARS-CoV-2.
(A) Multiplex assay of inflammatory cytokines in tissue lysates. For each panel, MM-O/N-0, MM-N-1, MM-N-4, MM-N-7, and MM-N-14 are shown in 1 column from left to right. The highest level of cytokine, set as 1, is used to normalize other samples within 1 panel, where the color density represents the relative levels of cytokines.

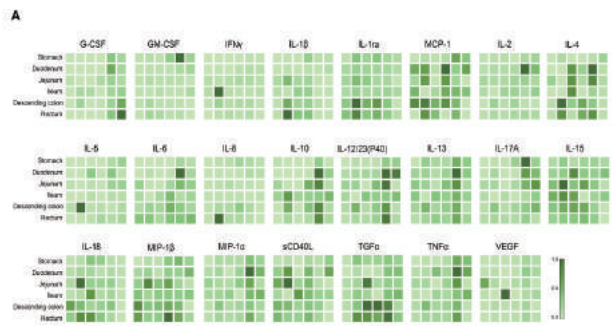

Figure 5. Inflammatory responses in the digestive system were induced by SARS-CoV-2 infection.
(A) Multiplex assay of inflammatory cytokines in digestive tissues. For each panel, MM-O/N-0, MM-O-1, MM-O-4, MM-O-7, and MM-O-14 are shown in 1 column from left to right. The highest level of cytokine, set as 1, is used to normalize the other samples within 1 panel, where the color density represents the relative levels of cytokines.

MILLIPLEX ®多因子试剂盒信息：

Non-Human Primate Cytokine/Chemokine Panel 1 (Cat. No. PCYTMG-40K-PX23)

Non-Human Primate Cytokine/Chemokine Panel 1

(Cat. No. PRCYTOMAG-40K)
(Cat. No. PCYTMG-40K-PX23)
(Bulk Cat. No. PRCYMAG40PMX23BK)

扫我咨询

sCD40L	IL-12/23 (p40)
G-CSF	IL-13
GM-CSF	IL-15
IFNγ	IL-17A/CTLA8
IL-1β	IL-18
IL-1Ra	MCP-1/CCL2
IL-2	MIP-1α/CCL3
IL-4	MIP-1β/CCL4
IL-5	TGFα
IL-6	TNFα
IL-8/CXCL8	VEGF-A
IL-10	

镁离子（Mg^{2+}）是生命所必需的。Mg^{2+} 是后生动物中最丰富的二价阳离子，是 ATP、核酸和无数代谢酶的必要辅助因子。研究人员通过全面的筛选，发现乳酸是细胞中 iMg^{2+} 的激活剂。在乳酸信号存在下，Mg^{2+} 从内质网中快速释放，促进多种细胞线粒体对 Mg^{2+} 的摄取。这一发现有望成为未来开发治疗心血管疾病、糖尿病等代谢性疾病的新型药物的跳板。

Lactate Elicits ER-Mitochondrial Mg^{2+} Dynamics to Integrate Cellular Metabolism

细胞动力学研究

Department of Medicine, Center for Precision Medicine, University of Texas Health San Antonio, San Antonio, USA
Received 11 March 2020, Revised 15 June 2020, Accepted 25 August 2020, Available online 8 October 2020.

Published: October 8, 2020
https://doi.org/10.1016/j.cell.2020.08.049

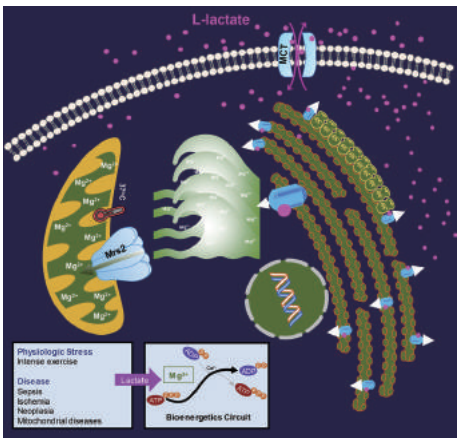

Abstract

Mg^{2+} is the most abundant divalent cation in metazoans and an essential cofactor for ATP, nucleic acids, and countless metabolic enzymes. To understand how the spatio-temporal dynamics of intracellular Mg^{2+} (iMg^{2+}) are integrated into cellular signaling, we implemented a comprehensive screen to discover regulators of iMg^{2+} dynamics. Lactate emerged as an activator of rapid release of Mg^{2+} from endoplasmic reticulum (ER) stores, which facilitates mitochondrial Mg^{2+} (mMg^{2+}) uptake in multiple cell types. We demonstrate that this process is remarkably temperature sensitive and mediated through intracellular but not extracellular signals. The ER-mitochondrial Mg^{2+} dynamics is selectively stimulated by L-lactate. Further, we show that lactate-mediated mMg2+ entry is facilitated by Mrs2, and point mutations in the intermembrane space loop limits mMg^{2+} uptake. Intriguingly, suppression of mMg^{2+} surge alleviates inflammation-induced multi-organ failure. Together, these findings reveal that lactate mobilizes

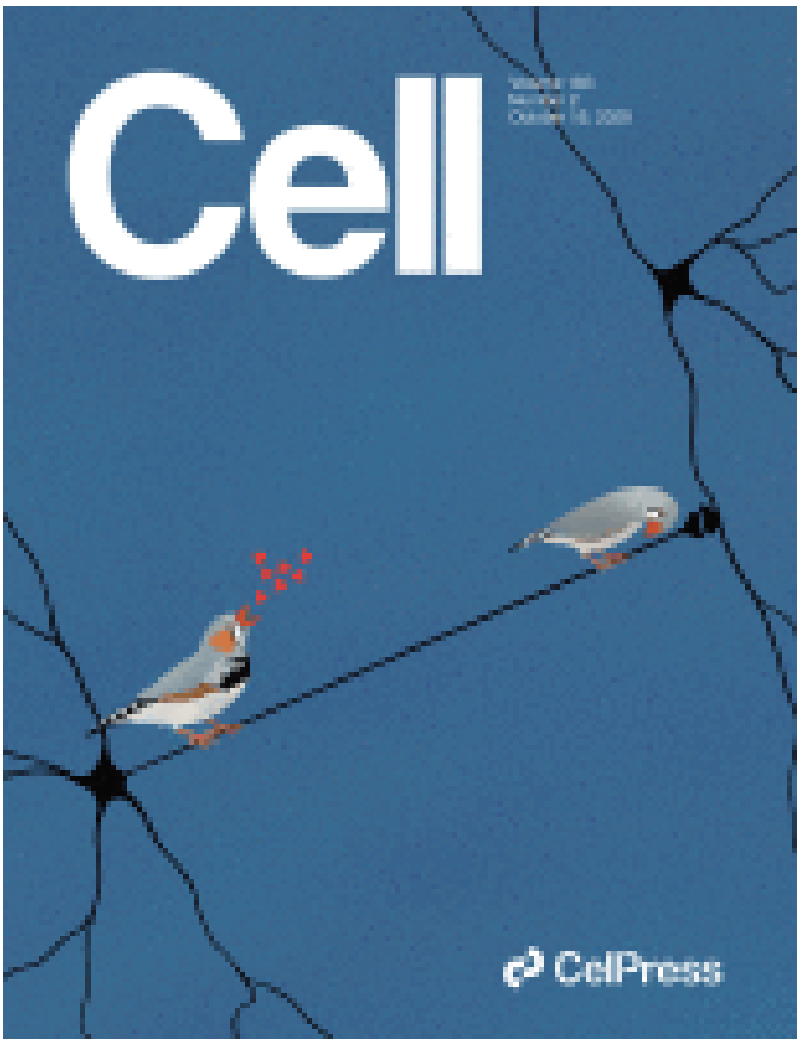

IF: 38.64

iMg^{2+} and links the mMg^{2+} transport machinery with major metabolic feedback circuits and mitochondrial bioenergetics.

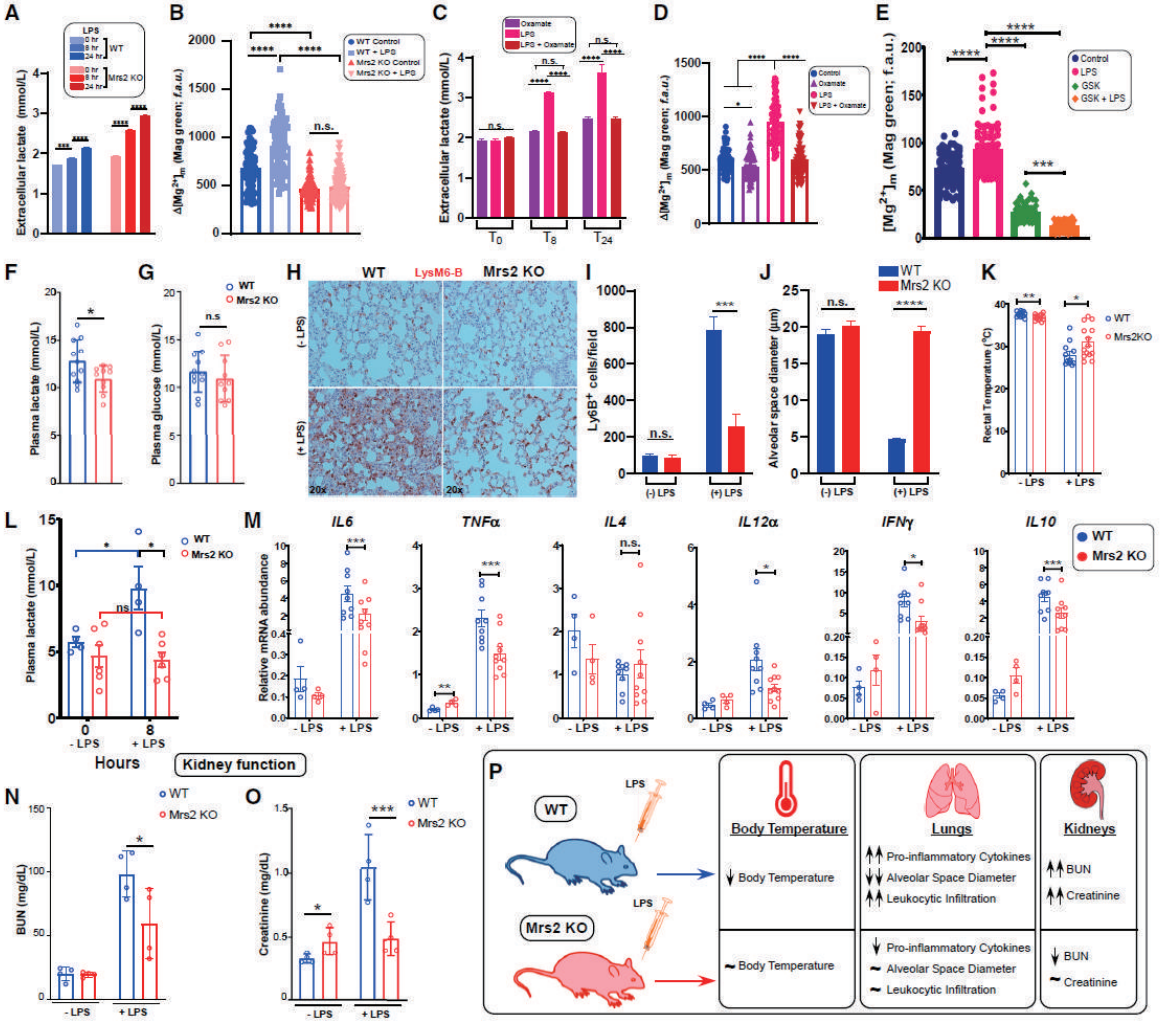

感染突变体rSARS-CoV-2的Calu-3细胞上清中IFN-b的浓度也降低

Figure 7. Growth kinetics and regulation of IFN-I response in wild-type and Nsp1 deletion virion
(G) Concentration of IFN-b in the supernatant of infected Calu-3 cells. Mean and SEM are shown. Significance betweenWT and mutant viruses was indicated; *p <0.05, **p < 0.01, and ***p < 0.001. Multiple t tests were performed.

MILLIPLEX ®多因子试剂盒信息：

Mouse Cytokine/Chemokine Panel 1

- (Cat. No. MCYTOMAG-70K)
- 25 (Cat. No. MCYTOMAG-70K-PMX)♦
- 25 (Bulk Cat. No. MCYTMAG70PMX25BK)♦
- 32 (Cat. No. MCYTMAG-70K-PX32)
- 32 (Bulk Cat. No. MCYTMAG70PMX32BK)

Eotaxin/CCL11	IL-13♦
G-CSF♦	IL-15♦
GM-CSF♦	IL-17A/CTLA8♦
IFNγ♦	IP-10/CXCL10♦
IL-1α♦	KC/GRO/CINC-1/ CXCL1♦
IL-1β♦	LIF
IL-2♦	LIX
IL-3	MCP-1/CCL2♦
IL-4♦	M-CSF
IL-5♦	MIG/CXCL9
IL-6♦	MIP-1α/CCL3♦
IL-7♦	MIP-1β/CCL4♦
IL-9♦	MIP-2/CXCL2♦
IL-10♦	RANTES/CCL5♦
IL-12 (p40)♦	TNFα♦
IL-12 (p70)♦	VEGF-A

扫我咨询

作者开发了一种多级策略分析神经干细胞功的不同状态 ，以鉴定调节其静止或激活水平的信号。利用细胞追踪、qPCR、多因子检测等手段，发现神经元状态之间的过渡发生在体内，证实了提高神经干细胞的警戒性的信号通路并提出干细胞可以对系统环境做出响应。采用 MILLIPLEX 多因子检测试剂盒对信号通路中的多种磷酸化蛋白进行检测，揭示了 TNF-α在调节神经干细胞进入和退出静止状态中的双重作用。

Adult Neural Stem Cells Are Alerted by Systemic Inflammation through TNF-a R Receptor Signalling

神经科学研究

Centro de Investigacio´ n Biome´ dica en Red sobre Enfermedades Neurodegenerativas (CIBERNED), Universidad de Valencia, Burjassot, Spain

Published: 4 February 2021
https://www.sciencedirect.com/science/article/abs/pii/S1934590920305105?via%3Dihub

Abstract

The SARS-CoV-2 virus, the causative agent of COVID-19, is undergoing constant mutation. Here, we utilized an integrative approach combining epidemiology, virus genome sequencing, clinical phenotyping, and experimental validation to locate mutations of clinical importance. We identified 35 recurrent variants, some of which are associated with clinical phenotypes related to severity. One variant, containing a deletion in the Nsp1-coding region (Δ500-532), was found in more than 20% of our sequenced samples and associates with higher RT-PCR cycle thresholds and lower serum IFN-β levels of infected patients. Deletion variants in this locus were found in 37 countries worldwide, and viruses isolated from clinical samples or engineered by reverse genetics with related deletions in Nsp1 also induce lower IFN-β responses in infected Calu-3 cells. Taken together, our virologic surveillance characterizes recurrent genetic diversity and identified mutations in Nsp1 of biological and clinical importance, which collectively may aid molecular diagnostics and drug design.

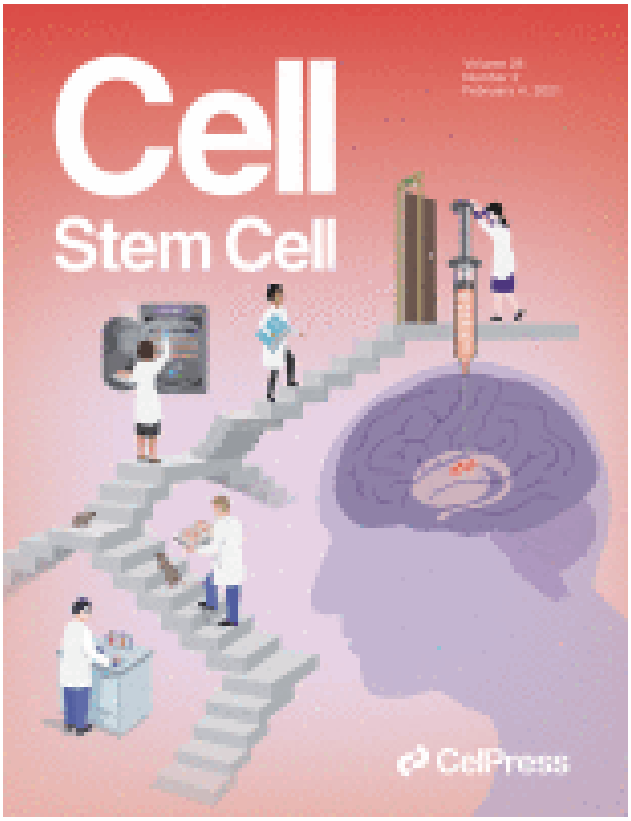

IF: 20.86

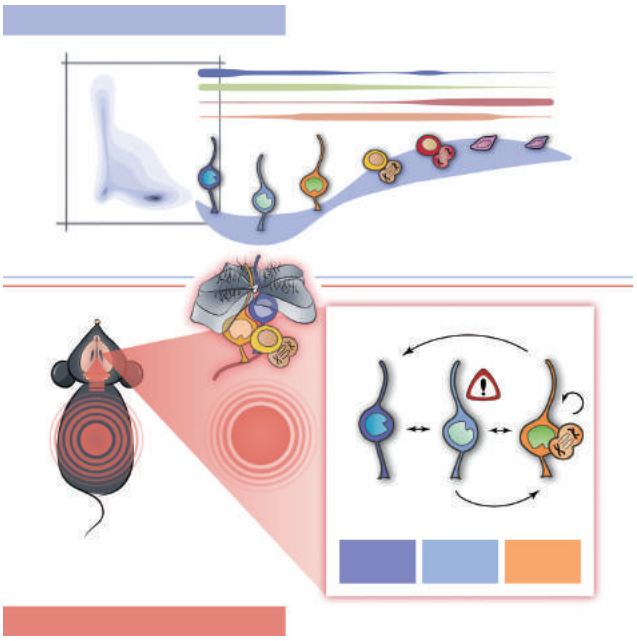

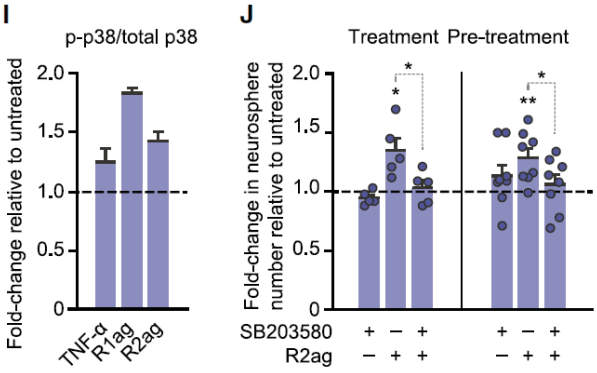

使用MILLIPLEX多因子检测试剂盒，对不同通路的磷酸化蛋白进行分析，发现TNFR1和TNFR2都能增加MAPK p38的磷酸化，TNFR2激动剂在神经球培养中的作用被特异性p38药物抑制剂SB203580所消除。

Figure 5. TNF-a Receptors Differentially Regulate NSCs In Vitro

(I) Quantification of phosphorylated levels of p38 relative to the total amount of the protein assessed after treatment (1 h) with R1ag or R2ag by Luminex-based multiplex assay. Data are normalized to untreated cells (n = 2).

(J) Number of wild-type neurospheres formed in the presence (treatment; left) or after pre-treatment (right) with R2ag and the p38 inhibitor SB203580. Data are represented relative to untreated controls.

All graphs show mean ± SEM. *p < 0.05, **p < 0.01, and ***p < 0.001.

MILLIPLEX ®多因子试剂盒信息：

Multi-Pathway (Phosphoprotein) — 9 Plex

(Cat. No. 48-680MAG) AB2 ▼ NON-CONFIGURABLE KIT

Analyte	Total	Phosphorylated	
Akt/PKB		3 (Ser473)	H, M, R
CREB		3 (Ser133)	H, M, R
Erk/MAPK 1/2		3 (Thr185/Tyr187)	H, M, R
JNK/SAPK1		3 (Thr183/Tyr185)	H, M, R
NFκB		3 (Ser536)	H, M
p38/SAPK2A/B		3 (Thr180/Tyr182)	H, M, R
p70S6 Kinase		3 (Thr389/412)	H, M, R
STAT3		3 (Ser727)	H, M, R
STAT5A/B		3 (Tyr694/699)	H, M, R

Multi-Pathway (Total) — 9 Plex

(Cat. No. 48-681MAG) AB2 ▼ NON-CONFIGURABLE KIT

Analyte	Total	Phosphorylated	
Akt/PKB	3		H, M, R
CREB	3		H, M, R
Erk/MAPK 1/2	3		H, M, R
JNK/SAPK1	3		H, M, R
NFκB	3		H, M, R
p38/SAPK2A/B	3		H, M, R
p70S6 Kinase	3		H, M, R
STAT3	3		H, M, R
STAT5A/B	3		H, M, R

扫我咨询

文章研究了食用核桃降低心血管疾病的机制，通过 MILLIPLEX® 多因子检测技术，检测了对照组人群和食用核桃的人群的血浆中多种炎症因子在两年内的变化，发现含核桃的饮食可以显著的降低多种炎症因子的含量，从而揭示了食用核桃降低心血管疾病的一种新的作用机制。

Effects of 2-Year Walnut-Supplemented Diet on Inflammatory Biomarkers

心血管疾病研究

Center for Nutrition, Healthy Lifestyle, and Disease Prevention School of Public Health
Loma Linda University

Published: November 10, 2020
https://doi.org/10.1016/j.cell.2020.08.049

Abstract

Nut consumption may be associated with lower CVD risk because nuts have a consistent cholesterollowering effect. A meta-analysis of 24 randomized controlled trials (RCTs) concluded that, compared with control diets, walnut-enriched diets resulted in significant weighted mean differences in low-density lipoprotein cholesterol (5.5 mg/dl), but had no effect on blood pressure or high-sensitivity C-reactive protein (hs-CRP) (2). Nut-enriched diets also affect endothelial function, with weighted mean differences in flow-mediated dilatation of 0.79% in 8 RCTs (3). These modest salutary effects of nut diets, however, cannot fully account for the lower CVD outcomes observed in prospective studies. Given the prevailing theory that inflammation is a major driver of atherosclerosis, 1 potential mechanism linking nut consumption to reduced CVD might be diminished inflammation.

IF: 20.59

TABLE 1 Baseline Concentrations and Changes in Circulating Inflammatory Biomarkers by Intervention Group

Biomarker	Walnut Diet (n = 324)	Control Diet (n = 310)	p Value*
GM-CSF, pg/ml			
Baseline	18.2 (16.4 to 20.0)	17.9 (16.0 to 19.9)	0.837
Change	−2.10 (−2.89 to −1.31)	−0.002 (−0.81 to 0.82)	<0.001
Percent change	−11.5 (−15.9 to −7.2)	−0.01 (−4.5 to 4.6)	
IFN-γ, pg/ml			
Baseline	16.2 (15.4 to 17.0)	15.2 (14.3 to 16.0)	0.083
Change	−1.35 (−1.81 to −0.89)	−0.09 (−0.55 to 0.38)	<0.001
Percent change	−8.3 (−11.2 to −5.5)	−0.6 (−3.6 to 2.5)	
IL-1β, pg/ml			
Baseline	1.19 (1.12 to 1.26)	1.14 (1.08 to 1.21)	0.354
Change	−0.12 (−0.16 to −0.08)	−0.02 (−0.06 to 0.02)	<0.001
Percent change	−10.1 (−13.4 to −6.7)	−1.8 (−5.3 to 1.8)	
IL-6, pg/ml			
Baseline	2.26 (2.09 to 2.44)	2.16 (1.98 to 2.33)	0.395
Change	−0.19 (−0.30 to −0.08)	−0.01 (−0.12 to 0.10)	0.021
Percent change	−8.4 (−13.3 to −3.5)	−0.5 (−5.6 to 4.6)	
TNF-α, pg/ml			
Baseline	6.09 (5.89 to 6.29)	5.86 (5.64 to 6.08)	0.135
Change	−0.40 (−0.57 to −0.24)	−0.09 (−0.26 to 0.08)	0.009
Percent change	−6.6 (−9.4 to −3.9)	−1.5 (−4.4 to 1.4)	
sE-selectin, ng/ml			
Baseline	49.4 (46.4 to 52.4)	47.1 (44.1 to 50.0)	0.277
Change	−1.66 (−2.67 to −0.65)	0.91 (−0.13 to 1.95)	0.001
Percent change	−3.5 (−5.6 to −1.5)	1.8 (−0.4 to 4.0)	
sICAM-1, ng/ml			
Baseline	1.37 (1.27 to 1.46)	1.24 (1.18 to 1.30)	0.037
Change	0.01 (−0.05 to 0.07)	0.03 (−0.03 to 0.09)	0.674
Percent change	1.5 (−2.9 to 5.1)	3.2 (−1.6 to 8.1)	
sVCAM-1, ng/ml			
Baseline	9.38 (9.14 to 9.63)	9.20 (8.96 to 9.44)	0.302
Change	−0.07 (−0.22 to 0.08)	0.04 (−0.11 to 0.20)	0.305
Percent change	−0.6 (−2.2 to 1.0)	0.7 (−1.1 to 2.3)	
SAA, ng/ml			
Baseline	106.9 (94.1 to 119.7)	106.6 (96.0 to 117.2)	0.970
Change	−2.40 (−11.12 to 6.31)	3.23 (−5.68 to 12.14)	0.377
Percent change	−2.2 (−10.4 to 5.9)	3.0 (−5.3 to 11.4)	
hs-CRP, mg/l			
Baseline	2.91 (2.22 to 3.60)	3.25 (2.62 to 3.88)	0.471
Change	−0.01 (−0.06 to 0.04)	−0.003 (−0.05 to 0.05)	0.903
Percent change	−2.8 (−19.6 to 14.1)	1.9 (−13.2 to 17.2)	

Values are mean (95% confidence interval). *Obtained by analysis of covariance of the change variables, adjusting for center, age, sex, hypertension, diabetes, education years, smoking, baseline statin use, in-trial statin changes, baseline body mass index, in-trial body mass index change, baseline physical activity, in-trial physical activity changes, and baseline cytokine values.

GM-CSF = granulocyte-monocyte colony stimulating factor; hs-CRP = high-sensitivity C-reactive protein; IFN = interferon; IL = interleukin; SAA = serum amyloid A; sE-selectin = soluble E-selectin; sICAM = soluble intercellular adhesion molecule; sVCAM = soluble vascular cell adhesion molecule; TNF = tumor necrosis factor.

与对照组相比，核桃饮食显著降低了检测的10个生物标志物中的6个指标。

Table 1 Baseline Concentrations and Changes in Circulating Inflammatory Biomarkers by Intervention Group

特应性皮炎（AD）是一种常见的皮肤病，影响全球 20% 的人口，具有显著的临床异质性。研究人员每隔 4 周对 AD 组和健康对照组的皮肤微生物进行全基因组分析，确定不同微生物组结构；采集血液样本进行免疫分析，对 AD 患者持续炎症水平进行研究。文章使用 MILLIPLEX® 多因子检测试剂盒对血清中 50 种生物标志物进行检测，发现 7 种分析物的水平仅在 B 型皮肤病患者中显著高于对照组（CCL17、CCL13、CCL22、CCL26、IL-13、TNF-B 和 S100A9）；另外，4 种分析物在 A 型和 B 型皮肤病患者中表现出显著的 TH2（CCL17，CCL22）和先天性（CCL13，CCL26）反应差异。

Atopic dermatitis microbiomes stratify into ecologic dermotypes enabling microbial virulence and disease severity

过敏，特异性皮炎研究

Skin Research Institute of Singapore, Agency of Science Technology and Research Institutes, Singapore

Available online 8 October 2020
https://doi.org/10.1016/j.jaci.2020.09.031

Abstract

Background: Atopic dermatitis (AD) is a common skin disease affecting up to 20% of the global population, with significant clinical heterogeneity and limited information about molecular subtypes and actionable biomarkers. Although alterations in the skin microbiome have been described in subjects with AD during progression to flare state, the prognostic value of baseline microbiome configurations has not been explored. Our aim was to identify microbial signatures on AD skin that are predictive of disease fate.

Methods: Nonlesional skin of patients with AD and healthy control subjects were sampled at 2 time points separated by at least 4 weeks. Using whole metagenome analysis of skin microbiomes of patients with AD and control subjects (n = 49 and 189 samples), we identified distinct microbiome configurations (dermotypes A and B). Blood was collected for immunophenotyping, and skin surface samples were analyzed for correlations with natural moisturizing factors and antimicrobial peptides.

Results: Dermotypes were robust and validated across 2 additional cohorts (63 individuals), with strong enrichment of subjects with AD in dermotype B. Dermotype B was characterized by reduced microbial richness, depletion of Cutibacterium acnes, Dermacoccus and Methylobacterium species, individual-specific outlier abundance of Staphylococcus species (eg, S epidermidis, S capitis, S aureus), and enrichment in metabolic pathways (eg, branched chain amino acids and arginine biosynthesis) and virulence genes (eg, β-toxin, δ-toxin) that defined a pathogenic ecology. Skin surface and circulating host biomarkers exhibited a distinct microbial-associated signature that was further reflected in more severe itching, frequent flares, and increased disease severity in patients harboring the dermotype B microbiome.

Conclusion: We report distinct clusters of microbial profiles that delineate the role of microbiome configurations in AD heterogeneity, highlight a mechanism for ongoing inflammation, and provide prognostic utility toward microbiome-based disease stratification.

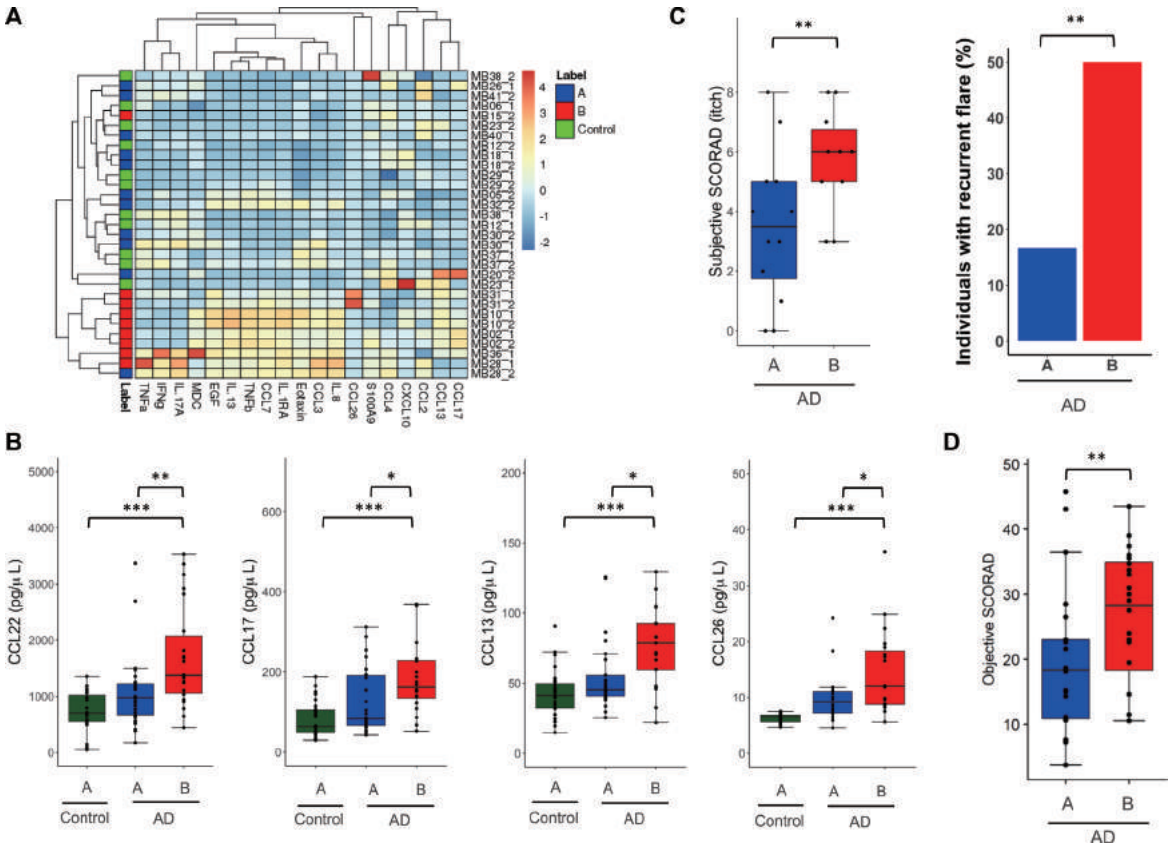

Fig 5. Systemic and phenotypic differences in dermotype B patients. A, Clustering based on AD-associated serum biomarker revealed a cluster of dermotype.

MILLIPLEX ®多因子试剂盒信息：

Human Cytokine/Chemokine Panel I
(Cat. No. HCYTMAG-60K-PX41)

Human Cytokine/Chemokine Panel I

- (Cat. No. HCYTOMAG-60K)
- 29 (Cat. No. HCYTMAG-60K-PX29)
- 30 (Cat. No. HCYTMAG-60K-PX30)♦
- 38 (Cat. No. HCYTMAG-60K-PX38)
- 41 (Cat. No. HCYTMAG-60K-PX41)

扫我试用

sCD40L	IL-9
EGF♦	IL-10♦
Eotaxin/CCL11♦	IL-12 (p40)♦
FGF-2/FGF-basic	IL-12 (p70)♦
Flt3 Ligand	IL-13♦
Fractalkine/CX3CL1	IL-15♦
G-CSF♦	IL-17A/CTLA8♦
GM-CSF♦	IP-10/CXCL10♦
GRO	MCP-1/CCL2♦
IFNα2♦	MCP-3/CCL7
IFNγ♦	MDC/CCL22
IL-1α♦	MIP-1α/CCL3♦
IL-1β♦	MIP-1β/CCL4♦
IL-1Ra♦	PDGF-AA▲
IL-2♦	PDGF-AB/BB ▲
IL-3♦	RANTES/CCL5♦▲
IL-4♦	TGFα
IL-5♦	TNFα♦
IL-6♦	TNFβ/Lymphotoxin-α (LTA)♦
IL-7♦	VEGF-A♦
IL-8/CXCL8♦	

文章探讨昼夜节律紊乱与多囊卵巢综合征（PCOS）的关系，建立了 PCOS 的大鼠模型，用 MILLIPLEX Rat Pituitary 试剂盒，对大鼠外周血多种激素进行了测定，结果发现夜班工作与多囊卵巢综合征显著相关。

Association between circadian rhythm disruption and polycystic ovary syndrome

生殖医学

Women's Hospital, School of Medicine, Zhejiang University, Hangzhou, China

Published Jan 04, 2021
https://doi.org/10.1016/j.fertnstert.2020.10.031

Abstract

Objective: To explore the association of circadian rhythm disruption with polycystic ovary syndrome (PCOS) and the potential underlying mechanism in ovarian granulosa cells (GCs). Design: Multicenter questionnaire-based survey, in vivo and ex vivo studies. Setting: Twelve hospitals in China, animal research center, and research laboratory of a women's hospital. Patients/Animals: A total of 436 PCOS case subjects and 715 control subjects were recruited for the survey. In vivo and ex vivo studies were conducted in PCOS-model rats and on ovarian GCs collected from women with PCOS and control subjects. Intervention(s): The PCOS rat model was established with the use of testosterone propionate. Main Outcome Measure(s): Assay for transposase-accessible chromatin with high-throughput sequencing (ATAC-seq), RNA sequencing, rhythmicity analysis, functional enrichment analysis. Result(s): There was a significant correlation between night shift work and PCOS. PCOS-model rats presented distinct differences in the circadian variation of corticotropin-releasing hormone, adrenocorticotropic hormone, prolactin, and a 4-h phase delay in thyrotropic hormone levels. The motif enrichment analysis of ATAC-seq revealed the absence of clock-related transcription factors in specific peaks of PCOS group, and RNA sequencing ex vivo at various time points over 24 hours demonstrated the differential rhythmic expression patterns of women with PCOS. Kyoto Encyclopedia of Genes and Genomes analysis further highlighted metabolic dysfunction, including both carbohydrate and amino acid metabolism and the tricarboxylic acid cycle. Conclusion(s): There is a significant association of night shift work with PCOS, and genome-wide chronodisruption exists in ovarian GCs.

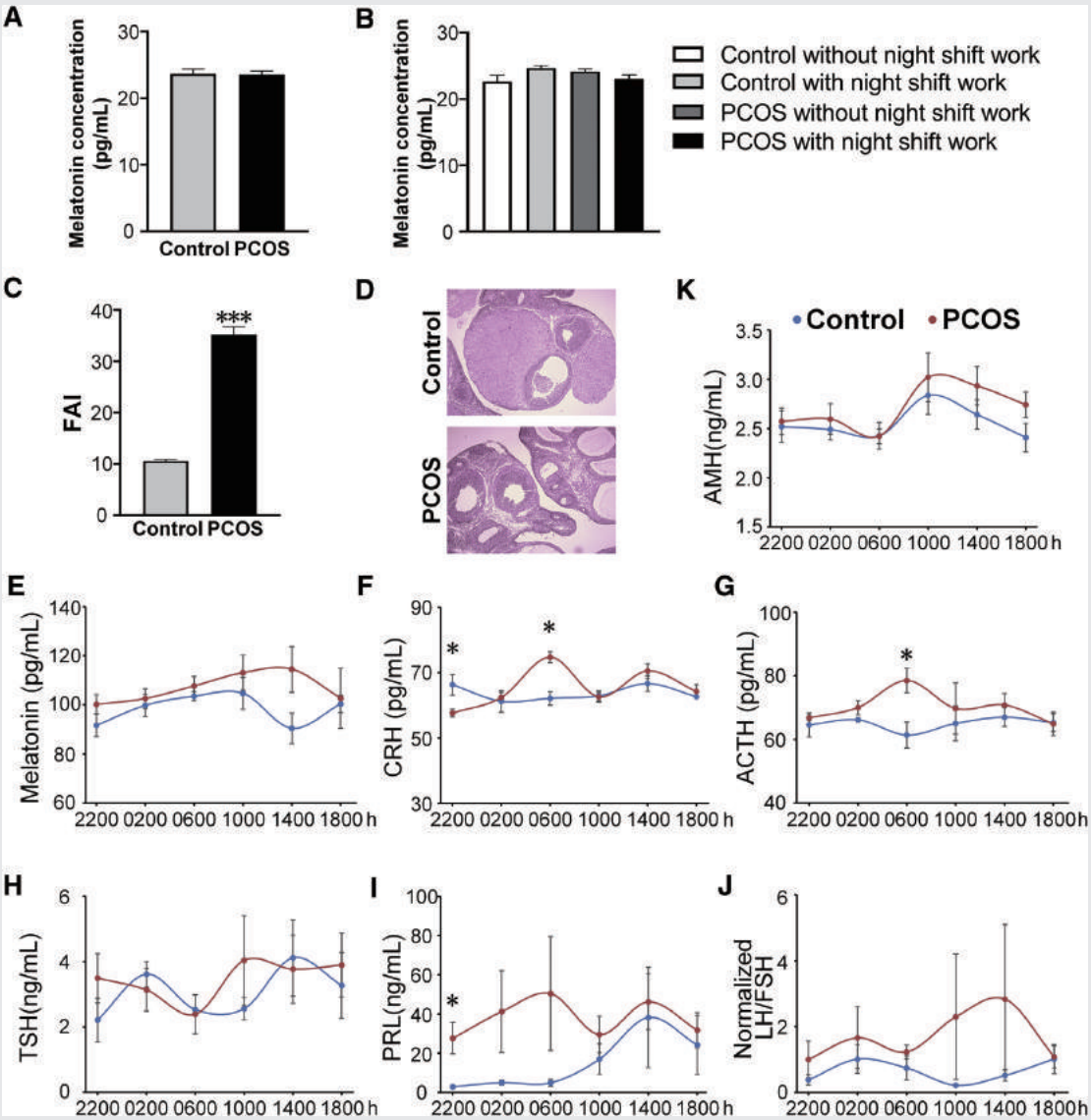

Circadian variation of peripheral hormone levels in PCOS and control subjects. (**A**) The serum melatonin levels of women with PCOS and controls (n = 36 in each group). (**B**) Detailed subgroups analysis (n = 18 in each group). (**C**) Serum free androgen index (FAI) of PCOS (n = 8) and control (n = 7) rats. (**D**) Rat ovarian histological examination using HE staining, with ×5 magnification. (**E–K**) Circadian variation of peripheral hormone levels in PCOS and control rats (n = 5 for each group): (**E**) melatonin, (**F**) corticotropin-releasing hormone (CRH), (**G**) adrenocorticotropic hormone (ACTH), (**H**) thyrotrophic hormone (TSH), (**I**) prolactin (PRL), (**J**) LH/FSH, (**K**) antimüllerian hormone (AMH). Data presented as mean ± SEM. Unpaired two-tailed Student *t* test, one-way analysis of variance, and the Bonferroni post test were performed for the data. *P*<.05 was considered to be statistically significant. PCOS = polycystic ovary syndrome.

Wang. Circadian rhythm disruption and PCOS. Fertil Steril 2020.

结果显示，与对照组大鼠相比，PCOS 大鼠的 CRH 水平在上午 6:00 时显著升高，在上午 10:00 时显著降低；PRL 水平在晚上 22:00 时显著升高。差异最明显的时间段是早上 6 点，此时 PCOS 大鼠 CRH 和 ACTH 水平达到峰值，此时正常组大鼠 CRH 和 ACTH 处于低谷。

Figure 1 Circadian variation of peripheral hormone levels in PCOS and control subjects. (E) melatonin, (F) corticotropin-releasing hormone (CRH), (G) adrenocorticotropic hormone (ACTH), (H) thyrotrophic hormone (TSH), (I) prolactin (PRL), (J) LH/FSH, (K) antim€ullerian hormone (AMH). Data presented as mean SEM. Unpaired two tailed Student t test, one-way analysis of variance, and the Bonferroni post test were performed for the data. P<.05 was considered to be statistically significant. PCOS ¼ polycystic ovary syndrome.

不同的细胞因子在妊娠的不同阶段可能发挥不同的作用，着床的初始阶段以促炎性而非抗炎性变化为特征，在这个关键点上，转变免疫调节，或许可以预防排斥半移植胚胎移植和成功建立妊娠。作者利用多因子检测手段比较受孕和非受孕女性的囊胚期胚胎移植后外周炎症相关因子的变化水平，发现在移植后第 3 天，血清促炎性细胞因子（IFN-γ和 IL-17）有短暂而适度的增加，随后消炎细胞因子（IL-10 和 TGF-β1）增加。

Successful implantation is associated with a transient increase in serum pro-inflammatory cytokine profile followed by a switch to anti-inflammatory cytokine profile prior to confirmation of pregnancy

生殖医学

The Chinese University of Hong Kong

Published: November 30, 2020
https://doi.org/10.1016/j.fertnstert.2020.10.031

Abstract

Objective: To compare the changing peripheral levels of inflammation-related cytokine profile during a 9-day period after blastocyst transfer between women who did and did not conceive. Design: Prospective, observational, and longitudinal study. Setting: University-affiliated hospital. Patient(s): Forty-seven women with infertility who were undergoing single day-5 blastocyst transfer were recruited. Intervention(s): This prospective observational and longitudinal study on 47 women with infertility was performed in an in vitro fertilization unit from December 2018 to August 2019. The amounts of a range of cytokines was measured on serial blood samples obtained during a 9-day period after blastocyst transfer. Main Outcome Measure(s): Serial blood samples were obtained on the day of embryo transfer, and 3, 6, and 9 days afterward for measurement of serum interferon gamma (IFN-g), tumor necrosis factor alpha, interleukin (IL)-2, IL-4, IL-10, IL-12, IL-13, IL-17, IL-18, and IL-22 using cytometric bead arrays; transforming growth factor beta 1 (TGF-b1) was measured using commercial enzyme-linked immunosorbent assay kits. Result(s): The cytokine profile was similar between the women who conceived and those who did not on the day of blastocyst transfer. In women who conceived, IFN-g and IL-17 (pro-inflammatory cytokines) exhibited a transient and significant increase on day 3 after blastocyst transfer, which decreased to the baseline levels by day 6. Meanwhile, IL-10 (anti-inflammatory cytokine) was increased significantly on days 6 and 9, and TGF-b1 (anti-inflammatory cytokine) was increased significantly on day 9 after blastocyst transfer. In women who did not conceive, there was a more pronounced increase in IFN-g and IL-17 (pro-inflammatory cytokines) on day 3, which was sustained on days 6 and 9 without a switch to an anti-inflammatory cytokine profile.

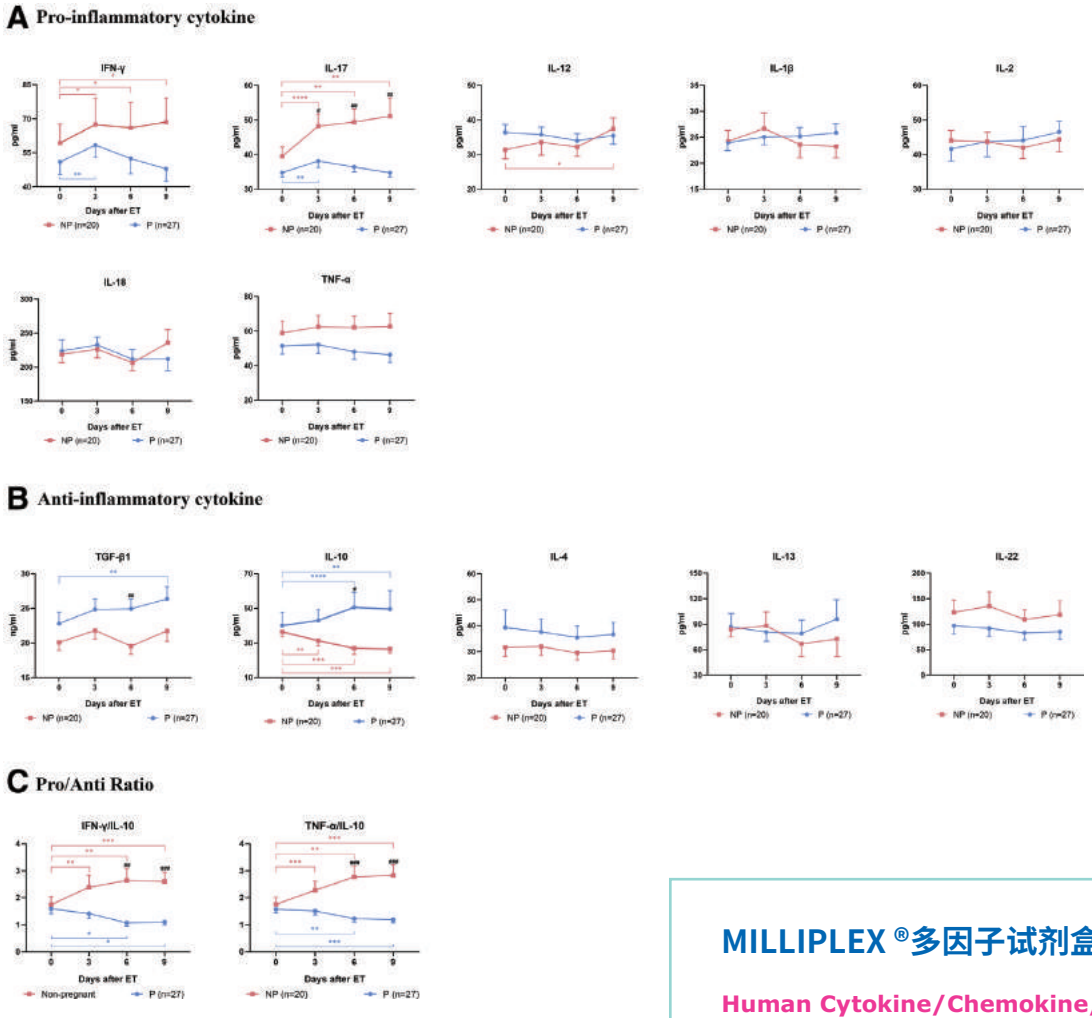

在胚胎移植当天和移植后 3、6、9 天采集系列血样，囊胚移植当天受孕妇女和未受孕妇女的细胞因子谱相似。在怀孕妇女中，IFN-g 和 IL-17（促炎细胞因子）在胚泡移植后第 3 天表现出短暂而显著的增加，到第 6 天下降到基线水平。同时，IL-10（抗炎细胞因子）在移植后第 6 天和第 9 天显著升高，TGF-b1（抗炎细胞因子）在移植后第 9 天显著升高。在未怀孕的妇女中，IFN-g 和 IL-17（促炎细胞因子）在第 3 天有更明显的增加，在第 6 天和第 9 天持续增加，而没有转换到抗炎细胞因子水平。

Figure 1. A comparison of the changing levels of peripheral cytokine parameters on the day of embryo transfer (ET) and on days 3, 6, and 9 after ET between women who did or did not conceive after ET. The results shown represent mean and standard error for peripheral cytokines and selected ratios on the day of ET (ET t 0) and 3, 6, and 9 days after ET (days ET t 3, t6, andt9, respectively). Y-axis is serum cytokine concentration (pg/mL or ng/mL). NP ?nonpregnant group (n=20); P ?pregnant group (n=27). Unpaired t test was used to compare the pregnant and nonpregnant groups; #P<.05; ##P<.01; ###P<.001. Paired t tests were used to compare the baseline level and sequential changes after ET separately for each group of women; *P<.05; **P<.01; ***P<.001; ****P<.0001. IFN= interferon; IL =interleukin; TGF=transforming growth factor; TNF= tumor necrosis factor.

MILLIPLEX ®多因子试剂盒信息：

Human Cytokine/Chemokine/ Growth Factor Panel A

- (Cat. No. HCYTA-60K)
- 38 (Cat. No. HCYTA-60K-PX38)♦
- 48 (Cat. No. HCYTA-60K-PX48)

扫我试用

sCD40L	IL-13♦
EGF♦	IL-15♦
Eotaxin/CCL11♦	IL-17A/CTLA8♦
FGF-2/FGF-basic	IL-17E/IL-25♦
Flt3 Ligand	IL-17F♦
Fractalkine/CX3CL1	IL-18♦
G-CSF♦	IL-22♦
GM-CSF♦	IL-27
GROα	IP-10/CXCL10♦
IFNα2♦	MCP-1/CCL2♦
IFNγ♦	MCP-3/CCL7
IL-1α♦	M-CSF♦
IL-1β♦	MDC/CCL22
IL-1RA♦	MIG/CXCL9♦
IL-2♦	MIP-1α/CCL3♦
IL-3♦	MIP-1β/CCL4♦
IL-4♦	PDGF-AA♦
IL-5♦	PDGF-AB/BB♦
IL-6♦	RANTES/CCL5♦▲
IL-7♦	TGFα
IL-8/CXCL8♦	TNFα♦
IL-9	TNFβ/Lymphotoxin-α (LTA)♦
IL-10♦	VEGF-A♦
IL-12 (p40)♦	
IL-12 (p70)♦	

远处转移是影响局部晚期直肠癌患者预后的主要因素。本研究旨在探讨新辅助放化疗（nCRT）联合手术后血液肿瘤突变负荷（bTMB）对局部晚期结肠癌（LARC）患者预后的影响。研究发现 bTMB 有可能改善治疗前和治疗后的风险评估，促进个体化治疗 LARC 患者的治疗。

Tumor mutation burden in blood predicts benefit from neoadjuvant chemo/ radiotherapy in locally advanced rectal cancer

结肠癌研究

Key laboratory of Carcinogenesis and Translational Research (Ministry of Education), Department of Gastrointestinal Surgery III, Peking University Cancer Hospital & Institute, China

Published: January 2021
https://doi.org/10.1016/j.ygeno.2020.10.029

Abstract

Distant metastasis has been the major concern of prognosis in patients with locally advanced rectal cancer (LARC). The purpose of this study was to investigate the prognostic value of TMB in blood (bTMB) in LARC patients after receiving neoadjuvant chemoradiotherapy (nCRT) and surgery. Using targeted ctDNA sequencing, we revealed that bTMB level at baseline was positively correlated with recurrence-free survival (RFS). Following nCRT, the patients with decreasing TMB tends to have a longer median RFS. bTMB level after surgery was negatively correlated with RFS. The serum cytokines including IFNγ, IFNα2, IL-1β, IL-2 and MIP-1β were significantly higher in pre-nCRT serum with higher bTMB group than that of lower bTMB group. Clonal evolution analysis showed that the pre- and post-nCRT ctDNAs of most cases had shared mutations. In conclusion, we presume that bTMB could potentially improve pre- and post-treatment risk assessment and facilitate individualized therapy for patients with LARC.

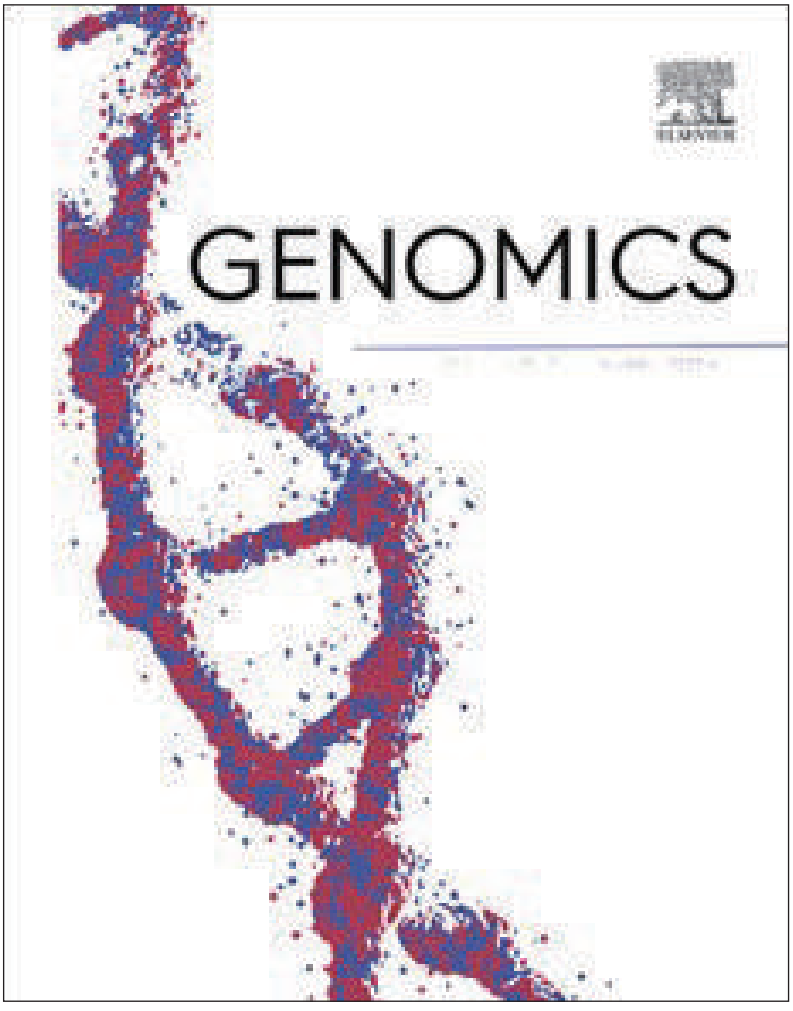

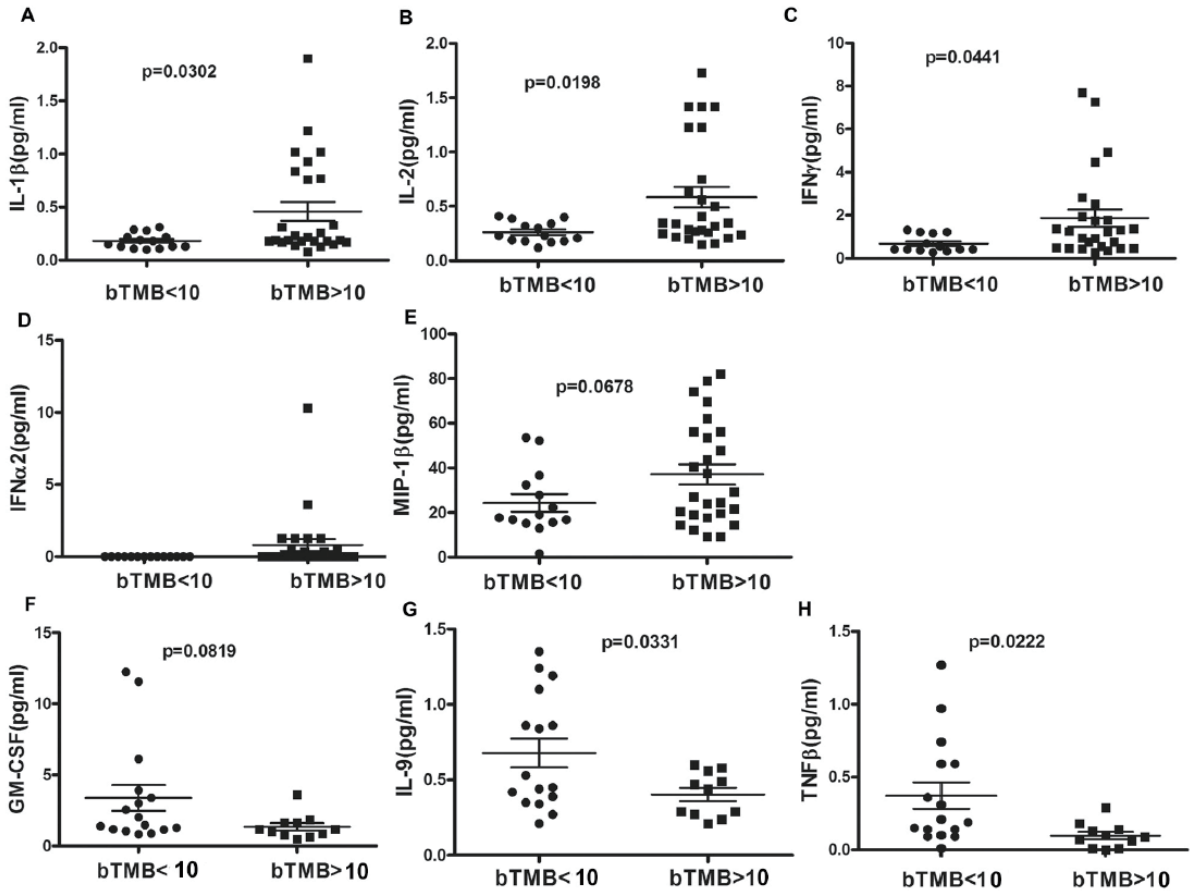

使用 MILLIPLEX 38 因子试剂盒，对局部晚期结肠癌 (LARC) 患者 (nCRT 前处理组，手术后组) 的血清进行炎症 / 趋化因子水平。结果发现，nCRT 前处理组 LARC 患者血清 IFNγ, IFNα2, IL-1β, IL-2 和 MIP-1β因子具高浓度现象，且伴随高 bTMB 水平(bTMB 值大于 10)。而手术后 LARC 患者血清 TNFFβ, IL-9 和 GM-CSF 具有高浓度现象，且伴随低 bTMB 水平 (bTMB 值小于 10)。结合 nCRT 治疗后组的绝大部分 LARC 病患出现 bTMB 水平下降现象，可推测出 nCRT 治疗前后细胞 / 趋化因子变化模式，可辅助 bTMB 判断新辅助化 / 放疗前后的风险,促进 LARC 患者的个体化治疗。

Fig. 5. The serum cytokine/chemokine levels and bTMB. (A-E) Compare the serum cytokine/chemokine levels between baseline bTMB<10 and bTMB>10 groups. (F–H) Compare the serum cytokine/chemokine levels between post-operation bTMB<10 and bTMB>10 groups.

MILLIPLEX ®多因子试剂盒信息：

Human Cytokine/Chemokine/ Growth Factor Panel A

38 (Cat. No. HCYTA-60K-PX38)♦

扫我试用

sCD40L	IL-13♦
EGF♦	IL-15♦
Eotaxin/CCL11♦	IL-17A/CTLA8♦
FGF-2/FGF-basic	IL-17E/IL-25♦
Flt3 Ligand	IL-17F♦
Fractalkine/CX3CL1	IL-18♦
G-CSF♦	IL-22♦
GM-CSF♦	IL-27
GROα	IP-10/CXCL10♦
IFNα2♦	MCP-1/CCL2♦
IFNγ♦	MCP-3/CCL7
IL-1α♦	M-CSF♦
IL-1β♦	MDC/CCL22
IL-1RA♦	MIG/CXCL9♦
IL-2♦	MIP-1α/CCL3♦
IL-3♦	MIP-1β/CCL4♦
IL-4♦	PDGF-AA♦
IL-5♦	PDGF-AB/BB♦
IL-6♦	RANTES/CCL5♦▲
IL-7♦	TGFα
IL-8/CXCL8♦	TNFα♦
IL-9	TNFβ/Lymphotoxin-α (LTA)♦
IL-10♦	VEGF-A♦
IL-12 (p40)♦	
IL-12 (p70)♦	

成功的异种细胞外基质再生医学策略需要炎症、纤维化和重塑过程之间的协同平衡。适应性巨噬细胞亚群已被确定调节炎症和协调邻近实质组织的修复。本研究制备了 PPARγ诱导的 CD68+CD206+M2 表型（M2γ），首次验证了它们在异种生物工程器官再生中的抗炎和组织再生作用。结果表明，体外 M2γ巨噬细胞能显著抑制 Th1 型 CD3+CD8+T 细胞对异种牙本质基质生物工程根复合体的反应。PPARγ的激活也及时地将 CD68+CD206+ 组织巨噬细胞极化为异种复合物。这些亚群减轻了炎症部位的促炎细胞因子（TNF-α、IFN-γ）和外周系统 CD3+CD8+T 淋巴细胞。当转化为原位非人灵长类动物模型时，PPARγ- 启动的 M2 巨噬细胞免疫抑制 IL-1β、IL-6、TNF-α、MMPs，使异种复合物有效地逃避免疫介导的排斥反应并启动移植物 - 宿主协同完整性。M1-M2 巨噬细胞的及时转化主要协调了成牙、成纤维和成骨，这是靶器官完整实质间质组织再生的潜在调节剂。

Recruited CD68+CD206+ macrophages orchestrate graft immune tolerance to prompt xenogeneic-dentin matrix-based tooth root regeneration

口腔材料科学

State Key Laboratory of Oral Diseases, West China Hospital of Stomatology, Sichuan University, Chengdu, China

Available online 14 October 2020
https://doi.org/10.1016/j.bioactmat.2020.09.029

Abstract

Successful regenerative medicine strategies of xenogeneic extracellular matrix need a synergistic balance among inflammation, fibrosis, and remodeling process. Adaptive macrophage subsets have been identified to modulate inflammation and orchestrate the repair of neighboring parenchymal tissues. This study fabricated PPARγ- primed CD68+CD206+ M2 phenotype (M2γ), and firstly verified their anti-inflammatory and tissue-regenerating roles in xenogeneic bioengineered organ regeneration. Our results showed that Th1-type CD3+CD8+ T cell response to xenogeneic-dentin matrix-based bioengineered root complex (xeno-complex) was significantly inhibited by M2γ macrophage in vitro. PPARγ activation also timely recruited CD68+CD206+ tissue macrophage polarization to xeno-complex in vivo. These subsets alleviated proinflammatory cytokines (TNF-α, IFN-γ) at the inflammation site and decreased CD3+CD8+ T lymphocytes in the periphery system. When translated to an orthotopic nonhuman primate model, PPARγ-primed M2 macrophages immunosuppressed IL-1β, IL-6, TNF-α, MMPs to enable xeno-complex to effectively escape immune-mediated rejection and initiate graft-host synergistic integrity. These collective activities promoted the differentiation of odontoblast-like and periodontal-like cells to guide pulp-dentin and cementum-PDLs-bone regeneration and rescued partially injured odontogenesis such as DSPP and periostin expression. Finally, the regenerated root showed structure-biomechanical and functional equivalency to the native tooth. The timely conversion of M1-to-M2 macrophage mainly orchestrated odontogenesis, fibrogenesis, and osteogenesis, which represents a potential modulator for intact parenchymal-stromal tissue regeneration of targeted organs.

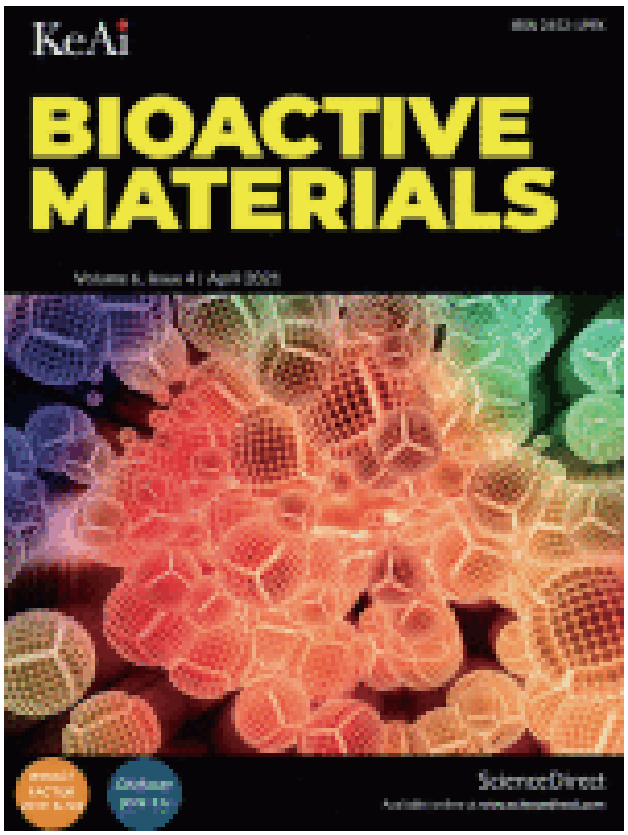

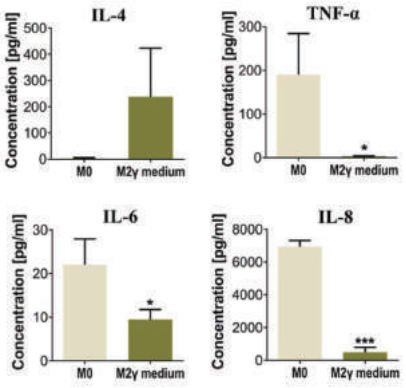

IL-4的高释放和IL-6、IL-8、肿瘤坏死因子-α（TNF-α）的低分泌确实揭示了M2γ培养基的抗炎能力

Fig. 2. M2γ macrophages suppressed the Th1-type CTL response triggered by xeno-complex in vitro. (C) Identification of M2γ conditional medium (M2γ medium). The anti-inflammatory and pro-inflammatory cytokines were analyzed using Immunology Multiplex MAP.

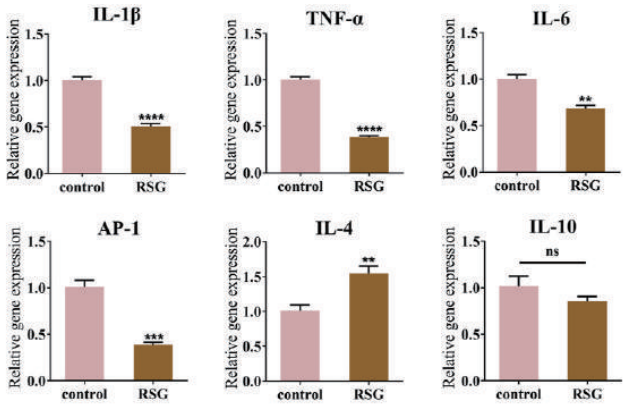

在异种复合物植入1周后，促炎细胞因子IL-1β、TNF-α、IL-6和AP-1在RSG治疗组中显著下调。

Fig. 5. PPARγ-primed macrophage inhibited acute inflammation after orthotopic implantation of xeno-complex in Non-human primates. (C) Th1/Th2-associated cytokines (IL-1β, TNF-α, IL-6, AP-1, IL-4, IL-10). All data are normalized to those of GAPDH mRNA and are presented relative to those of Control, set as 1. All data are mean ± SEM (n ≥ 3), **p < 0.01, ***p < 0.001, ****p < 0.0001. NS, no significance.

MILLIPLEX®多因子试剂盒信息：

Non-Human Primate Cytokine/Chemokine Panel 1 (Cat. No. PRCYTOMAG-40K)

Non-Human Primate Cytokine/Chemokine Panel 1

(Cat. No. PRCYTOMAG-40K)
(Cat. No. PCYTMG-40K-PX23)
(Bulk Cat. No. PRCYMAG40PMX23BK)

扫我咨询

sCD40L	IL-12/23 (p40)
G-CSF	IL-13
GM-CSF	IL-15
IFNγ	IL-17A/CTLA8
IL-1β	IL-18
IL-1Ra	MCP-1/CCL2
IL-2	MIP-1α/CCL3
IL-4	MIP-1β/CCL4
IL-5	TGFα
IL-6	TNFα
IL-8/CXCL8	VEGF-A
IL-10	

03 精彩瞬间

28 Jan 2021

Mary Young
Research Technician
University of Virginia,
School of Medicine

Webinar: IgG Antibodies Against SARS-CoV-2 Correlate to Days from Symptom Onset in COVID-19 Positive Patients

在本次网络研讨会中，您将了解：

- 新型 MILLIPLEX®SARS-CoV-2 抗原检测试剂盒，如何实现 SARS-CoV-2 抗原 (S1、S2、RBD 和 N 蛋白) 的 IgG、IgA 和 IgM 抗体水平检测
- 阳性患者治疗前后的抗体水平变化
- 抗体出现与患病天数的相关性。

18 Feb 2021

MILLIPLEX® Learning Center is now LIVE!

MILLIPLEX® 学习中心上线，在这里你可以找到 MILLIPLEX® 相关的产品介绍视频、网络研讨会视频、产品手册、应用海报等。为了让内容更容易找到，我们还根据研究领域对内容进行了分组，方便查阅。

18 May 2021

Alexandra Donlan
University of Virginia

Webinar: IL-13 is a Pathogenic Driver of COVID-19

对两个独立的 COVID-19 患者队列研究发现，白细胞介素 -13（IL-13）的增加与机械通气的需要有关。此外，服用 IL-13 和 IL-4 受体阻滞剂 dupilumab 可以有效减轻 COVID-19 的患者病情较轻。在 SARS-CoV-2 感染的小鼠中，抑制剂中和 IL-13 可大幅度降低疾病严重程度，证明了这种细胞因子的致病作用。白介素 13 阻断后，透明质酸合成酶 1 基因 Has1 被鉴定为高度下调的基因。此外，阻断透明质酸受体 CD44 可降低受感染小鼠的死亡率，表明该通路受 IL-13 调控。了解 IL-13 和透明质酸的作用对于 COVID-19 和潜在的其他肺部疾病的治疗具有重要意义。

在本次网络研讨会中，您将了解：

- 使用 MILLIPLEX® Human Cytokine/Chemokine/Growth Factor Panel A，同时分析 COVID-19 血浆样本中的 48 种免疫因子；
- 血浆分析物与 COVID-19 疾病参数的相关性，包括机械通气的需要；
- 2 型免疫应答，特别是 IL-13，如何在 COVID-19 严重性中发挥作用。

30 May 2021

MILLIPLEX合作服务平台年度认证培训

为了增强 MILLIPLEX® 检测服务能力，增强客户使用的便携度、满意度。2021 年 3 月底，在默克生命科学中国技术与合作中心举办举办了 MILLIPLEX® 合作服平台年度认证培训，期间默克技术专家对 MILLIPLEX® 试剂盒样本处理、试剂盒操作、上机读板、数据处理等过程，进行了细致的培训与考核。对每一位通过认证的学院颁发了认证证书。

您精准稳定实验的保证，源自默克生命科学全方位蛋白免疫检测解决方案

默克强大的生物标志物检测平台为您提供高通量，可同时检测多个生物标志物的 MILLIPLEX® 技术平台，还有经过多年验证业内金标准的代谢、神经研究相关 ELISA 检测试剂盒，还有新一代可检测浓度低至飞摩尔级别蛋白的超高灵敏度的 SMC™ (Single molecule counting) 单分子蛋白免疫检测平台。我们确保以最少的重复次数帮助您得到最为可靠的结果。

MILLIPLEX®多因子检测试剂盒

MILLIPLEX® 多因子免疫检测试剂盒，可以实现百种蛋白因子的同步检测。产品设计初衷就是最大限度的为客户节约时间、节约经费、节约样本。以最快的速度、最少的时间和最低的样本需求量，发最高质量的文章。

MILLIPLEX® 为您带来：

多： 1-500 重蛋白同时检测，百种蛋白因子可选
快： 自动化高通量，每小时数据量可达 9,600 个
好： 严格的质量控制保证批次间、批次内稳定性
省： 大大节约操作时间、样本数量、经费成本

SMCxPRO™
前所未有的超高灵敏度蛋白定量平台

科学家经常遇到仅有使用少量体积的血浆或血清进行生物标志物分析，这会涉及到对低丰度蛋白标志物进行快速精确的定量。默克新一代SMCxPRO™超高度敏感蛋白检测设备，能够完美与您的研究流程相结合，可以在您的样本中检测到低至飞摩尔级别含量的蛋白标志物，将您的代谢研究开拓至全新阶段。

SMCxPRO™可以为您带来：

- 超高灵敏度检测，检测极限可达 fg/mL
- 384 孔板高通量快速读取分析
- 设计精巧时尚，使用操作简单
- 支持定制化试剂与样本检测服务

ELISA
易于操作、结果稳定、数据可靠

默克ELISA产品覆盖了多种研究领域和物种，试剂盒全部经过严格验证，为您提供易于操作且稳定的ELISAs产品，帮助您得到可靠、可重复的结果，在复杂样品类型进行定量生物标志物检测可达到pg/mL水平。我们目前的ELISA产品超过1800多种，均具备高灵敏，并且特异性好的的特点。请登录**SigmaAldrich.com/ELISA**了解更多。

愈见清晰

默克 您的免疫检测专家
想您所想 助您见所未见

我们的免疫检测试剂盒开发生产具有严格的质控标准，让您对实验数据更有信心

严格的开发试剂盒过程

特异性

- 抗体特异性检测：检测在样本中被忽略的抗体和其他蛋白或者分析物之间的交叉反应
- 实验特异性检测：保障每一个因子在单独检测和多重检测时候的数据一致性

方法验证

- 比较同一种因子在不同的试剂盒中 (MILLIPLEX® ,ELISA或SMC™ assays), 以及与其他供应商试剂盒中同一种因子的表现。确保为您提供最佳表现的试剂盒

反应缓冲液优化

- 优化Assay buffer和微球稀释液，进而提高在基质中抗体与分析物的结合

检测灵敏度

- 每一种蛋白的检测范围和最小检测浓(minDCs)都可以在说明书中找到，这些数据是基于我们真实的样本中检测得到的数据

在样本基质中的表现

- 试剂盒在特定的样本类型，例如血清或者血浆中都已经过验证，我们也会提供优化的天然血清基质模拟样本中的环境

可重复的结果值得您信任

稳定性

- 所有的试剂盒都经过严苛的运输稳定性的测
- 测试样本在一定温度的范围内，即反复冻融后的待测因子的稳定性；如果样本有特殊的处理条件，会在说明书中进行标注

准确性

- 板内和板间误差在10-15%范围内
- 准确性评定范围通常是± 20%

线性稀释

- 对每种分析物在三种浓度下进行样品中的峰回收率;稀释后的样品结果必须与样品中分析物的浓度成正比，差异一般在±20%以内

批次间稳定性

- 有“金标准”的校准样本被用作所有未来生所有产批次的参考

专家技术支持

- 我们的销售专家、技术支持科学家、客户支持和免疫分析开发团队将在您需要的时候，为您提供专业的支持服务。

我们会帮助您选择合适的平台和实验满足您的需求，在未来我们也会与您一同合作满足您对实验平台以及数据质量的需求

我们诚挚
期待您最真实的反馈

如您有更多感兴趣的话题与方向；
如您已经在使用 MILLIPLEX® 试剂盒，有使用疑问；
请给我们留言，我们会在后期内容中不断完善。

如您有更多产品需求；
如您有产品讲座 / 试用需求；
请给我们留言，我们会第一时间回复信息。

如果您愿意分享您与 MILLIPLEX® 的故事与照片；
一句简答的使用评价、一张试剂盒的使用照片；
分享优质内容的读者，我们将寄出精美礼品。

留言方式：

扫描下方二维码，在打开界面点我留言中，后台会及时给你回复。

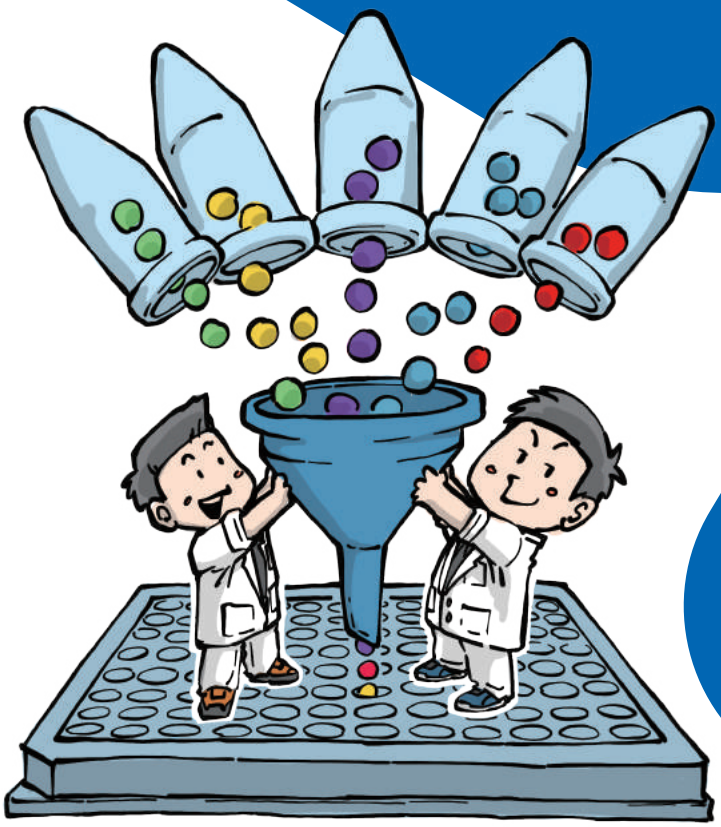

上海
上海市浦东新区东育路227弄3号
前滩世贸中心(二期)C栋15-18层
电话:(021)20338288
传真:(021)50803042
邮编:200126

北京
北京市朝阳区将台路甲2号
诺金中心25层
电话:(010)59072688
传真:(010)59072699
邮编:100016

广州
广州市天河区冼村路5号
凯华国际中心1201-1204
电话:(020)32255333
传真:(020)32255380
邮编:510623

成都
成都市锦江区人民南路二段1号
仁恒置地广场1706室
电话:(028)80740222
传真:(028)80740227
邮编:610016

默克生命科学技术服务热线：400 620 3333 或 400 889 1988转2号线
中国技术服务中心： tscn@merckgroup.com
更多详情，敬请登陆：www.merckmillipore.com www.sigmaaldrich.cn

资料编号：04/2021